MONITORED STEADY STATE EXCITATION AND RECOVERY (MSSER) RADIATION FORCE IMAGING OF ENGINEERED TISSUE CONSTRUCTS

Aaron Cole Richardson

A thesis submitted to the faculty of the University of North Carolina at Chapel Hill in partial fulfillment of the requirements for the degree of Master of Science in the Department of Biomedical Engineering

Chapel Hill
2010

Approved by:

Dr. Caterina Gallippi

Dr. Elizabeth Loboa

Dr. Mansoor Haider

ABSTRACT

AARON RICHARDSON: Monitored Steady State Excitation and Recovery (MSSER) Radiation Force Imaging of Engineered Tissue Constructs
(Under the direction of Caterina Gallippi)

Production of engineered bone tissue requires integration of synthetic and natural materials and ideal chemical and mechanical stimulation. More understanding of changes in mechanical properties of these tissues during differentiation is needed. Current tensile testing methods result in destruction of tissue constructs. A non-destructive testing method is desired. Monitor Steady State Excitation and Recovery, MSSER, an ultrasound imaging based elastography method, uses prolonged acoustic force to displace tissue while monitoring changes in strain during force application. MSSER, along with the underdamped harmonic oscillation model, was used to determine the elastic modulus of tissue constructs. Localized elastic modulus values were calculated using MSSER for tissue constructs grown in osteogenic and complete (non-osteogenic) growth media. Images showing elastic modulus values were produced. Validation of elastic modulus images were done performing calcium digestion on tissue constructs. MSSER hopes to provide a non-invasive testing method, allow for localized measurements, and aid in calcium detection.

ACKNOWLEDGEMENTS

I would like to take this opportunity to thank all of those who assisted with this study. First I would like to thank Audrey Charoenpanich for preparing the cells which were used in this study. I would next like to thank Mallory Scola for her assistance in production of the ultrasound beam sequences used in this study along with her assistance in setting up the experiments. Next, I would like to recognize Carla Haslauer for her assistance in performing the calcium digestion in this study. I would also like thank my committee members Elizabeth Loboa and Mansoor Haider for their guidance through this study. Finally, I would like to extent a special thanks to my advisor and committee chair, Caterina Gallippi, for her guidance, assistance, and many hours she dedicated to overseeing the completion of this study.

TABLE OF CONTENTS

LIST OF FIGURES

Figure

Chapter 1: Introduction and Thesis Overview

The research in this thesis investigates the usefulness of novel ultrasonic imaging methods to calculate the elastic modulus values of cell seeded collagen gel tissue constructs grown for osteogenic differentiation. Current methods for testing these tissue constructs are highly invasive and result in destruction of these construct. Therefore, it is desirable to develop a method which is non-invasive and allows for mechanical testing of these tissue constructs while they are growing in culture media.

In this study, novel ultrasonic imaging methods, developed for the use in elastography were explored as a method to provide a better solution for testing mechanical properties of these tissue constructs. The ultrasonic elastography imaging method used, Monitor Steady State Excitation and Recovery (MSSER), is a modified form of Acoustic Radiation Force Impulse (ARFI) imaging. MSSER applies a constant force while observing material creep to steady state displacement. Material response after force cessation may also be monitored. MSSER methods, which mimic a mechanical creep test, are used for testing viscoelastic materials due to changes in strain over time under constant force application. MSSER is capable of recording these changes in strain under constant force. Previous work with MSSER by Mauldin et. al. successfully used this imaging technique in conjunction with the Voigt and Standard Linear models of viscoelasticity to calculate the elastic modulus of viscoelastic materials.[1] It was found, however, that these models were not a good fit for

---

1. Mauldin, F. W. Jr., Haider, M. A., Loboa, E. G., Behler, R. H., Euliss, L. E., Pfeiler, T. W., Gallippi, C. M., "Monitored Steady-State Excitation and Recovery (MSSER) Radiation Force Imaging Using Viscoelastic Models" *IEEE Transaction on Ultrasonics, Ferroelectrics, and Frequency Control*,Vol. 55, No. 7, 2008, pp. 1597-1610.

characterizing these tissue constructs, since actual displacement curves did not match those produced by the models. This bad model fit was attributed to the size and shape of the tissue constructs being tested in addition to damped oscillation which occurs in these constructs at force cessation. The materials being tested were much different in size and shape than materials earlier tested. The thin string-like tissue constructs under tension attached to anchors on each side provided a unique challenge in imaging and required use of another model to better describe the behavior of these constructs. It was found the underdamped harmonic oscillation model better characterized the tissue construct responses during MSSER imaging, specifically the underdamped oscillation which occurred in the constructs after force cessation.

The elastic modulus was calculated using the spring or stiffness constant, a parameter extracted from the underdamped harmonic oscillation model. The oscillation frequency of the tissue construct along with the mass constant were two pieces of information calculated from MSSER data. This information, along with the acoustic force magnitude, was used to calculate the elastic modulus. The acceleration of the tissue during excitation, an important value used in the mass constant calculation, was calculated two different ways. (More information about tissue acceleration calculations may be found in Chapter 4.) Parametric images of elastic modulus values were successfully produced along with elastic modulus values reported. The values were compared to elastic modulus values calculated by Pfeiler et. al. in earlier work.[2] Although our preliminary data suggests that MSSER can be used for mechanical property testing of these tissue constructs, more work is needed to perfect these

---

2. Pfeiler, T. W., Sumanasinghe, R. D., Loboa, E. G., "Finite element modeling of 3D human mesenchymal stem cell-seeded collagen matrices exposed to tensile strain." *Journal of Biomechanics* Vol. 41, 2008, pp. 2289-2296.

methods.

This thesis contains information about the background, along with procedures and calculations. In addition, results are presented along with analysis of these results and [2] future directions for this study. Chapter 2 contains informaottion about ultrasonic imaging, along with novel ultrasonic technologies and information about the field of elastography. This chapter also discusses MSSER and its application to studying mechanical properties of the tissue constructs. Chapter 3 contains information on current tissue engineering techniques, along with information on the biomechanical properties of biological tissues. Methods for testing mechanical properties along with the harmonic oscillation model are discussed within this chapter. Chapter 4 consists of the methods and materials, including information on calculations and production of stiffness images. The results are compared to previous work along with comments on the results. Chapter 5 provides a summary along with future directions of this study.

2. Pfeiler, T. W., Sumanasinghe, R. D., Loboa, E. G., "Finite element modeling of 3D human mesenchymal stem cell-seeded collagen matrices exposed to tensile strain." *Journal of Biomechanics* Vol. 41, 2008, pp. 2289-2296.

1. Mauldin, F. W. Jr., Haider, M. A., Loboa, E. G., Behler, R. H., Euliss, L. E., Pfeiler, T. W., Gallippi, C. M., "Monitored Steady-State Excitation and Recovery (MSSER) Radiation Force Imaging Using Viscoelastic Models" *IEEE Transaction on Ultrasonics, Ferroelectrics, and Frequency Control*,Vol. 55, No. 7, 2008, pp. 1597-1610.

2. Pfeiler, T. W., Sumanasinghe, R. D., Loboa, E. G., "Finite element modeling of 3D human mesenchymal stem cell-seeded collagen matrices exposed to tensile strain." *Journal of Biomechanics* Vol. 41, 2008, pp. 2289-2296.

Chapter 2: Ultrasonic Imaging

Background on ultrasonic imaging

Ultrasound is a noninvasive, relatively inexpensive diagnostic medical imaging modality. Minimum stress and inconvenience to patients along with no use of any potentially harmful ionizing energy are other benefits of this technology.[1] Ultrasound is generally used to analyze internal organs, muscles, tendons, and detect pathological lesions. Since images are captured in real time, movement of organs can be seen along with blood flow though vessels.

Ultrasonic waves, generated by piezoelectric elements, used in the imaging process are on the frequency range of 2 to 15MHz and propagate through soft tissue at speeds of around 1540 m/s^2. The piezoelectric elements, located in the ultrasound transducer, convert electrical pulses into mechanical pulses and vise versa.[2] The pulses are a result of the piezoelectric effect which occurs when these crystals are exposed to a voltage potential. This electric potential results in a disruption of the crystal lattice causing a deformation to form in the crystal. This deformation results in the production of a pressure wave. These longitudinal pressure waves then travel into the tissue being examined. Once inside the tissue, these waves interact with the tissue. The waves are partially absorbed, reflected or scattered as they travel through the tissue. These interferences result in echoes that are reflected back to the transducer giving information about the tissue. The echo pulses are detected by piezoelectric crystals which transform the acoustic echoes into electrical pulses.

1. Lutz, H.T., Gharbi, H. A., Basics of Ultrasound. New York, NY. Spinger Berlin Heidelberg, 2006, pp1-19.
2 Jensen, Jorgen. "Medical ultrasound imaging" Progress in Biophysics and Molecular Biology. Vol. 93 (2007) 153-165.

Computer equipment processes the acquired data first by analyzing the echoes with respect to their site of origin. This is determined by the time-distance principle. The intensity of the received echoes is next determined. From this information, a black and white speckle image can be produced. The ultrasound waves are created and received by the same transducer. Transducers with different geometries along with different frequencies are available to meet various imaging needs. Most clinical ultrasound transducers are linear array transducers which have many elements capable of transmitting and receiving acoustic pulses. Using multiple elements along with delaying inner elements with respect to the outer elements allows for focusing of the ultrasound beam. A more focused ultrasound beam does not only provide clearer data, but penetrates deeper into tissue.

The focused ultrasound beam results in an ultrasonic field (Figure 1). This field encompasses the region below the ultrasound transducer in which the ultrasound beam travels. Three parts of the field exist and include the near field, the focus points, and the far field.[3] The resolution of this field can be characterized by the lateral, axial, and elevational resolutions. The lateral resolution is dependent upon the diameter of the ultrasound beam, axial resolution depends on the length of the emitted ultrasound pulse and pulse wavelength, and elevational resolution the thickness of the transducer element.[4]

---

3 Wells, P. N., "Ultrasound imaging" Phys. Med. Biol. Vol. **51** (2006) pp. R83-R98

4. Woo, J., "A short history of the development of Ultrasound in Obstetrics and Gynecology". 2002. Available (Online) http://www.ob-ultrasound.net/history1.html. Accessed March 12, 2010

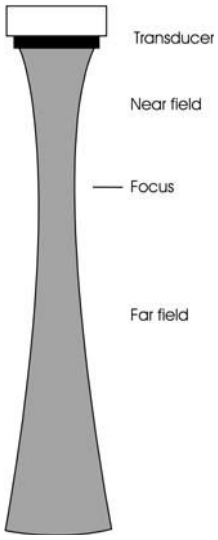

Figure 1 shows an approximation of an ultrasound field. Lateral direction of this field is left and right, axial direction is up and down, while elevational direction is in and out of the page. [3]

(Image by Lutz et. al[1])

Multiple ultrasound imaging modes exists. A-mode imaging, which appears in a one-dimensional waveform, is used to detect information about small or rapid movements. B-mode imaging is used to produce a cross-section anatomical image. This B-mode imaging is most commonly used in clinical applications. M-mode imaging, created from a succession of A-mode images, can show time-varying displacements. Another form of ultrasound imaging is Doppler imaging. This method uses the frequency or phase shift of sound which occurs for moving objects and determines the speed of the moving object. Doppler images are color coded showing not only the speed of moving objects within the body, such as blood, but also the direction of those objects.[5]

Background on elastography including acoustic radiation force methods

Palpation has long been used as a diagnostic tool for detecting disease based on the fact that pathologic changes alter the stiffness of tissue.

5. Prince, J. L., Links, J. M., Medical Imaging Signals and Systems. Pearson Prentice Hall: Upper Saddle River, NJ, 2006, Pp 11-12, 315-316.

These stiffness changes are a result of changes in the mechanical properties of tissue.[4,5,6] However, small lesion size or deep location within the body make it difficult to detect and characterize some lesions by palpation. Even though the elastic modulus of normal soft tissue ranges over as much as four orders of magnitude, this range dramatically increases in diseased tissue.[7]

The need for better methods of detection for these property changes accompanying disease has led to the creation of the field of elastography. The prevailing imaging modality used in this field of study has been ultrasound. However, conventional ultrasound is not capable of detecting such differences in mechanical properties, therefore novel ultrasound methods have been created.[6,8]

Many different elastography methods have been explored and developed. One such method is compression elastography in which tissue is imaged before and after a compression force is applied. Using correlation techniques, pre and post compression images are compared to render a strain map of the tissue.[9,10] Another form, transient elastography, uses low frequency vibration to create motion within the tissue. While tissue is in motion, pulse-echo ultrasound is used to detect tissue displacements.[8]

4. Greenleaf JF, Fatemi M, Insana M. Selected methods for imaging elastic properties of biological tissues. Annu Rev Biomed Eng 2003; 5:57–78.
5. Xydeas T, Siegmann K, Sinkus R, Krainick-Strobel U, Miller S, Claussen CD. Magnetic resonance elastography of the breast: correlation of signal intensity data with viscoelastic properties. Invest Radiol 2005; 40:412–420.
6. Glozman, T., Azhari, H., "A Method for Characterization of Tissue Elastic Properties Combining Ultrasound Computed Tomography With Elastography." J Ultrasound Med. Vol. 29 pp 387-398.
7. Sarvazyan A. 1993. Shear acoustic properties of soft biological tissues in medical diagnostics. *Proc. Acoust. Soc. Am.*, 125th, Ottawa, Canada, p. 2329
8. Gao L, Parker KJ, Lerner RM, Levinson SF. Imaging the elastic properties of tissue: a review. Ultrasound Med Biol 1996; 22:959–977.
9. Bercoff J, Chaffai S, Tanter M, et al. In vivo breast tumor detection using transient elastography. Ultrasound Med Biol 2003; 29:1387–1396.
10. Catheline S, Gennison JL, Delon O, et al. Measurements of viscoelastic properties of homogeneous soft solid using transient elastography: an inverse problem approach. J Acoust Soc Am 2004; 116:3734–3741

Most elastography methods rely on the principle that stiffer tissue will displace less than soft tissue when a stress is applied. Applied stress and displacement differences can provide important information regarding tissue properties and even be used in calculating parameters such as the elastic modulus.[6] All of the earlier mentioned external methods of applying compression forces lack the ability to apply the compression or excitation force directly to internal areas of interest. Therefore internal methods which are capable of applying a force directly to a region of interest and probing the tissue point by point have been investigated. Internal sources such as cardiac pulsation or breathing have been considered. A more reliable method of internal excitation being used and developed for elastography includes using the radiation force of ultrasound in which a beam of ultrasound is used to apply a stress to the tissue and measure resulting strains. Acoustic radiation force can penetrate boundaries giving information about regions of interest which are deep in tissue.[4,12]

Acoustic Radiation Force Impulse (ARFI) imaging is an ultrasound imaging system based on radiation force which provides information about the local mechanical properties of tissue. Differences in mechanical properties are detected via differences in tissue displacement when acoustic radiation force is applied. Recovery time of the displaced tissue provides additional information about mechanical properties. The displacements are monitored and tracked using ultrasound tracking correlation based methods. Such methods allow for both temporal and spatial tracking of displacements when acoustic force is applied.

---

4. Woo, J., "A short history of the development of Ultrasound in Obstetrics and Gynecology". 2002. Available (Online) http://www.ob-ultrasound.net/history1.html. Accessed March 12, 2010
6. Glozman, T., Azhari, H., "A Method for Characterization of Tissue Elastic Properties Combining Ultrasound Computed Tomography With Elastography." J Ultrasound Med. Vol. 29 pp 387-398.
12. Sarvazyan A, Rudenko OV, Swanson SD, Fowlkes JB, Emelianov Y. 1998. Shear wave elasticity imaging: a new ultrasonic technology of medical diagnostics. *Ultrasound Med. Biol.* 24(9):1419–35

This acoustic radiation force occurs due to the propagation of acoustic waves through dissipative media. As sound waves are dissipated through media, momentum is transferred to the tissue. Ultimately, the transfer of momentum applied to the focal region of the ultrasonic beam results in the application of a body force. This force is applied in the same direction as the wave traveling through media[13]. In media absorbing an ultrasound wave, the magnitude of the force can be calculated by the following equation

$$F = \frac{Wabsorbed}{c} = \frac{2\alpha I}{c}$$

where F is defined as the acoustic force measured in N/m^3, α is defined as the attenuation coefficient measure in units of Np/m, I is the temporal average intensity in units of W/m^2. [13,14,15,16] The shape of this intensity field can be described by a dimensionless quantity referred to as the f-number (F/#). This (F/#) is calculated by the following relation:

$$F/\# = \frac{z}{d}$$

13. Nightingale, K., Soo, M. S., Nightingale, R., Trahey, G., "Acoustic Radiation Force Impulse Imaging: In Vivo Demonstration of Clinical Feasiblity." *Ultrasound in Medicine and Biology*. Oct 24, 2001
14. Torr, G. The acoustic radiation force. Am. J. Phys. 52:402 408, 1984.
15. Nyborg, W. Acoustic streaming. In: Mason, W., ed., Physical Acoustics, New York: Academic Press Inc, vol. IIB, chap. 11, 265{331. 1965.
16. Nightingale, K., McAleavey, S., Trahey, G., "Shear-Wave Generation Using Acoustic Radiation Force: *In Vivo* and *Ex Vivo* Results" Ultrasound in Med and Biol. Vol 29 No. 12, 2003, pp. 1715-1723.

Where d is the aperture width and z is the acoustic focal length. This configuration results in a body force applied throughout the tissue within the geometric shadow of the transducer. The transducer produces a variable-magnitiude body force.[17,18, 19] The dynamic response of tissue to this acoustic force is indicative of the mechanical properties of the tissue.[17] Magnitude displacement is inversely related to the stiffness of the tissue. Stiffer tissue produces less displacement than softer tissue under acoustic radiation force. These differences in displacement indicate variations in the elastic modulus within tissue being imaged. Differences in tissue stiffness properties from normal tissue are often associated with pathological tissue.

ARFI imaging may be performed using a diagnostic ultrasound scanner and clinical ultrasound transducer, which produce both the acoustic radiation force and measures the resulting displacements. The same transducer is used to apply the acoustic force and measure the resulting displacement using B-mode tracking pulses.[17] Use of the same transducer eliminates any issues with alignment and makes clinical use easier and more realistic when performing ARFI. The force application can be customized by changing the transmitter pulse shape along with the temporal profile and period. The duration of the force, usually less then 1 millisecond, can also be adjusted.[13]

Ultrasonic methods for measuring mechanical properties or stiffness of tissue are clinically relevant due to stiffness changes which occur during disease.[20]

---

13. Nightingale, K., Soo, M. S., Nightingale, R., Trahey, G., "Acoustic Radiation Force Impulse Imaging: In Vivo Demonstration of Clinical Feasiblity." *Ultrasound in Medicine and Biology*. Oct 24, 2001
17. Palmeri, M.L., Sharma, A. C., Bouchard, R. R., Nightingale, R. W., Nightingale, K. R., "A Finite-Element Method Model of Soft Tissue Response to Impulsive Acoustic Radiation Force." *IEEE Transaction on Ultrasonics, Ferroelectrics, and Frequency Control,* Vol 52. No. 10, 2005, Pp 1699-1711.
18. A. Sarvazyan, O. Rudenko, S. Swanson, J. Fowlkes, and S. Emelianov, "Shear wave elasticity imaging: A new ultrasonictechnology of medical diagnostics," *Ultrasound Med. Biol.*, vol. 24, no. 9, pp. 1419–1435, 1998.
19. O. Rudenko, A. Sarvazyan, and S. Emelianov, "Acoustic radiation force and streaming induced by focused nonlinear ultrasound in a dissipative medium," *J. Acoust. Soc. Amer.*, vol. 99, no. 5, pp. 2791–2798, 1996.
20. Nightingale, K.R., Palmeri, M.L., Nightingale, R. W., Trahey, G. E., "On the feasibility of remote palpation using acoustic radiation force*." J. Acoust. Soc Am* Vol. 110, 2001.

Differences in tissue displacement can give critical information about pathologies that may exist.[13] ARFI imaging has been successfully used in elastography studies. The advantage ARFI provides in elastography is the application of the force and subsequent measurement of stiffness can be applied to areas superficial to boundary layers.[17,20]

Prolonged acoustic radiation force application: Monitored Steady State Excitation and Recovery (MSSER) Ultrasound

ARFI uses short (~ 70 microseconds) excitation pulses, which give information regarding tissue response to impulsive excitation only. In materials which strain is time dependent, impulsive excitation does not give an accurate displacement value. Therefore, prolonged acoustic force applications have been studied. Such techniques are useful in studying steady state displacement of tissue. One prolonged force application that has been developed is called Kinetic Acoustic Vitreoretinal Examination (KAVE). KAVE is an application of ARFI imaging which was developed for imaging of the vitreous membrane of the eye. This technique uses multiple acoustic pulses generated by a single element piston transducer. As a result small, localized displacements are generated.[21] At cessation of force, transient tissue response is measured. This technique allows for monitoring the steady state tissue response when a constant force is applied. KAVE imaging allows for determination of maximum displacement, relative viscosity, and relative elasticity.

---

13. Nightingale, K., Soo, M. S., Nightingale, R., Trahey, G., "Acoustic Radiation Force Impulse Imaging: In Vivo Demonstration of Clinical Feasiblity." *Ultrasound in Medicine and Biology*. Oct 24, 2001
17. Palmeri, M.L., Sharma, A. C., Bouchard, R. R., Nightingale, R. W., Nightingale, K. R., "A Finite-Element Method Model of Soft Tissue Response to Impulsive Acoustic Radiation Force." *IEEE Transaction on Ultrasonics, Ferroelectrics, and Frequency Control,* Vol 52. No. 10, 2005, Pp 1699-1711.
20. Nightingale, K.R., Palmeri, M.L., Nightingale, R. W., Trahey, G. E., "On the feasibility of remote palpation using acoustic radiation force*." J. Acoust. Soc Am* Vol. 110, 2001.
21. Mauldin, F. W. Jr., Haider, M. A., Loboa, E. G., Behler, R. H., Euliss, L. E., Pfeiler, T. W., Gallippi, C. M., "Monitored Steady-State Excitation and Recovery (MSSER) Radiation Force Imaging Using Viscoelastic Models" *IEEE Transaction on Ultrasonics, Ferroelectrics, and Frequency Control*,Vol. 55, No. 7, 2008, pp. 1597-1610.

These mechanical property values are useful in characterizing the vitreous membrane. This technology promises to be useful in detecting mechanical property changes as a result of diseases which occur in this membrane.[22,23]

Another form of ARFI imaging called Monitored Steady State Excitation and Recovery (MSSER) also shows promising uses in elastography. This method uses an extended force application to monitor the steady state displacement of tissue. It can also be used to monitor the responses at cessation of the force application. MSSER techniques mimic a creep test by applying a constant force and observing the change in strain of the material over time. MSSER has already shown potential in being useful for testing the mechanical properties of tissues with viscoelastic properties. It has already been successfully used in conjunction with the Voigt and Standard Linear models of viscoelastic materials to determine mechanical properties such as the Elastic modulus and viscosity.[21] An advantage MSSER provides over KAVE is that it allows for monitoring the transient response of the tissue constructs at force cessation. This response, such as tissue oscillation frequency, at force cessation is an important parameter used in the elastic modulus calculation.

MSSER: Nondestructive testing of the mechanical properties of engineered tissue

The main advantage MSSER gives over current techniques for measuring the elastic modulus is that it can be done non-invasively. Current methods require removal of

---

21. Mauldin, F. W. Jr., Haider, M. A., Loboa, E. G., Behler, R. H., Euliss, L. E., Pfeiler, T. W., Gallippi, C. M., "Monitored Steady-State Excitation and Recovery (MSSER) Radiation Force Imaging Using Viscoelastic Models" *IEEE Transaction on Ultrasonics, Ferroelectrics, and Frequency Control*,Vol. 55, No. 7, 2008, pp. 1597-1610.
22. W. F. Walker, F. J. Fernandez, and L. A. Negron, "A method of imaging viscoelastic parameters with acoustic radiation force," *Phys. Med. Biol.*, vol. 45, no. 6, pp. 1437–1447, 2000.
23. F. Viola and W. F. Walker, "Radiation force imaging of viscoelasticproperties with reduced artifacts," *IEEE Trans. Ultrason.,Ferroelect., Freq. Contr.*, vol. 50, no. 6, pp. 736–742, 2003.

constructs from growth media and subsequent death of the cells.

These current methods use a tensile test which results in the destruction of tissue construct being tested. The use of a tensile test is a loss of resources and time.[26] Current testing methods are discussed more in Chapter 3. MSSER would allow testing of mechanical properties to occur while the tissue constructs are still alive growing in culture media.

MSSER also shows potential for being more accurate than the current method. Finite Element Analysis (FEA) is used to try and predict elastic modulus differences within the tissue constructs. This analysis assumes the tissue construct has linear elastic properties.[26] MSSER, designed for testing of viscoelastic materials, allows for a point by point analysis of the tissue constructs. For example, with this technology, it would be possible to detect focal areas of calcium deposition or hardening along these constructs. Although FEA is also capable of predicting local strains using a globally obtained elastic modulus value and geometric parameters of the construct, MSSER is capable of performing localized measurements along the tissue constructs. This also includes measurements at multiple depths within the tissue construct.

Conclusion

Ultrasound imaging, a dynamic imaging modality, is highly utilized within the clinical setting to study anatomy and detect disease.[27] Being relatively inexpensive, portable, and able to provide real time information has lead to much research in finding additional methods of use for this imaging modality.

26. Pfeiler, T. W., Sumanasinghe, R. D., Loboa, E. G., "Finite element modeling of 3D human mesenchymal stem cell-seeded collagen matrices exposed to tensile strain." *Journal of Biomechanics* Vol. 41, 2008, pp. 2289-2296.
27.Lutz, H.T., Gharbi, H. A., Basics of Ultrasound. New York, NY. Spinger Berlin Heidelberg, 2006, pp1-19.

Ultrasound technology has been utilized in the growing field of elastography. Being able to examine the mechanical properties of biological tissue will be advantageous in the detection of diseases, such as cancer or cardiovascular disease, in which these are accompanied by changes in tissue stiffness. Ultrasound is a desirable tool to use in elastography due to radiation force's ability to penetrate boundaries allowing for examination of tissue that is not close to the surface.[28,29,30] ARFI has been developed to administer an acoustic radiation force to produce tissue displacements which can be measured along with the time it takes for the tissue to recover back to its steady state location.[31] Another benefit of MSSER is it allows for focal measurements localized to regions that span hundreds of microns. This is in contrast to the current method in which an average elastic modulus value is taken over a large range of tissue. MSSER, a modification of ARFI, allows for a prolonged force application rather than an instantaneous force. MSSER also allows for tracking of changes in tissue displacement over time while force is being applied along with monitoring recovery time or any oscillations that occur after tissue excitation. ARFI is only capable of measuring impulsive force response of tissue and not steady state displacement. MSSER, which mimics a creep test, can be used to measure mechanical properties of viscoelastic materials, which experience changes in strain over time with the application of a constant force.

---

28. Greenleaf JF, Fatemi M, Insana M. Selected methods for imaging elastic properties of biological tissues. Annu Rev Biomed Eng 2003; 5:57–78.
29. Xydeas T, Siegmann K, Sinkus R, Krainick-Strobel U, Miller S, Claussen CD. Magnetic resonance elastography of the breast: correlation of signal intensity data with viscoelastic properties. Invest Radiol 2005; 40:412–420.
30. Glozman, T., Azhari, H., "A Method for Characterization of Tissue Elastic Properties Combining Ultrasound Computed Tomography With Elastography." J Ultrasound Med. Vol. 29 pp 387-398.

1. Lutz, H.T., Gharbi, H. A., Basics of Ultrasound. New York, NY. Spinger Berlin Heidelberg, 2006, pp1-19.

2 Jensen, Jorgen. "Medical ultrasound imaging" Progress in Biophysics and Molecular Biology. Vol. 93 (2007) 153-165.

3 Wells, P. N., "Ultrasound imaging" Phys. Med. Biol. Vol. **51** (2006) pp. R83-R98

4. Woo, J., "A short history of the development of Ultrasound in Obstetrics and Gynecology". 2002. Available (Online) http://www.ob-ultrasound.net/history1.html. Accessed March 12, 2010

5 Prince, J. L., Links, J. M., Medical Imaging Signals and Systems. Pearson Prentice Hall: Upper Saddle River, NJ, 2006, Pp 11-12, 315-316.

4. Greenleaf JF, Fatemi M, Insana M. Selected methods for imaging elastic properties of biological tissues. Annu Rev Biomed Eng 2003; 5:57–78.

5. Xydeas T, Siegmann K, Sinkus R, Krainick-Strobel U, Miller S, Claussen CD. Magnetic resonance elastography of the breast: correlation of signal intensity data with viscoelastic properties. Invest Radiol 2005; 40:412–420.

6. Glozman, T., Azhari, H., "A Method for Characterization of Tissue Elastic Properties Combining Ultrasound Computed Tomography With Elastography." J Ultrasound Med. Vol. 29 pp 387-398.

7. Sarvazyan A. 1993. Shear acoustic properties of soft biological tissues in medical diagnostics. *Proc. Acoust. Soc. Am.*, 125th, Ottawa, Canada, p. 2329

8. Gao L, Parker KJ, Lerner RM, Levinson SF. Imaging the elastic properties of tissue: a review. Ultrasound Med Biol 1996; 22:959–977.

9. Bercoff J, Chaffai S, Tanter M, et al. In vivo breast tumor detection using transient elastography. Ultrasound Med Biol 2003; 29:1387–1396.

10. Catheline S, Gennison JL, Delon O, et al. Measurements of viscoelastic properties of homogeneous soft solid using transient elastography: an inverse problem approach. J Acoust Soc Am 2004; 116:3734–3741.

11. Taylor LS, Porter BC, Rubens DJ, Parker KJ. Three-dimensional sonoelastography: principles and practices. Phys Med Biol 2000; 45:1477–1494.

12. Sarvazyan A, Rudenko OV, Swanson SD, Fowlkes JB, Emelianov Y. 1998. Shear wave elasticity imaging: a new ultrasonic technology of medical diagnostics. *Ultrasound Med. Biol.* 24(9):1419–35

13. Nightingale, K., Soo, M. S., Nightingale, R., Trahey, G., "Acoustic Radiation Force Impulse Imaging: In Vivo Demonstration of Clinical Feasiblity." *Ultrasound in Medicine and Biology*. Oct 24, 2001

14. Torr, G. The acoustic radiation force. Am. J. Phys. 52:402 408, 1984.

15. Nyborg, W. Acoustic streaming. In: Mason, W., ed., Physical Acoustics, New York: Academic Press Inc, vol. IIB, chap. 11, 265{331. 1965.

16. Nightingale, K., McAleavey, S., Trahey, G., "Shear-Wave Generation Using Acoustic Radiation Force: *In Vivo* and *Ex Vivo* Results" Ultrasound in Med and Biol. Vol 29 No. 12, 2003, pp. 1715-1723.

17. Palmeri, M.L., Sharma, A. C., Bouchard, R. R., Nightingale, R. W., Nightingale, K. R., "A Finite-Element Method Model of Soft Tissue Response to Impulsive Acoustic Radiation Force." *IEEE Transaction on Ultrasonics, Ferroelectrics, and Frequency Control,* Vol 52. No. 10, 2005, Pp 1699-1711.

18. A. Sarvazyan, O. Rudenko, S. Swanson, J. Fowlkes, and S. Emelianov, "Shear wave elasticity imaging: A new ultrasonictechnology of medical diagnostics," *Ultrasound Med. Biol.*, vol. 24, no. 9, pp. 1419–1435, 1998.

19. O. Rudenko, A. Sarvazyan, and S. Emelianov, "Acoustic radiation force and streaming induced by focused nonlinear ultrasound in a dissipative medium," *J. Acoust. Soc. Amer.*, vol. 99, no. 5, pp. 2791–2798, 1996.

20. Nightingale, K.R., Palmeri, M.L., Nightingale, R. W., Trahey, G. E., "On the feasibility of remote palpation using acoustic radiation force*." J. Acoust. Soc Am* Vol. 110, 2001.

21. Mauldin, F. W. Jr., Haider, M. A., Loboa, E. G., Behler, R. H., Euliss, L. E., Pfeiler, T. W., Gallippi, C. M., "Monitored Steady-State Excitation and Recovery (MSSER) Radiation Force Imaging Using Viscoelastic Models" *IEEE Transaction on Ultrasonics, Ferroelectrics, and Frequency Control*,Vol. 55, No. 7, 2008, pp. 1597-1610.

22. W. F. Walker, F. J. Fernandez, and L. A. Negron, "A method of imaging viscoelastic parameters with acoustic radiation
force," *Phys. Med. Biol.*, vol. 45, no. 6, pp. 1437–1447, 2000.

23. F. Viola and W. F. Walker, "Radiation force imaging of viscoelasticproperties with reduced artifacts," *IEEE Trans. Ultrason.,Ferroelect., Freq. Contr.*, vol. 50, no. 6, pp. 736–742, 2003.

24. Lakes,Roderic, Viscoelastic Materials, Cambridge University Press 2008 pp 1.5
New York, New York.

25. Mauldin, F. W. Jr., Haider, M. A., Loboa, E. G., Behler, R. H., Euliss, L. E., Pfeiler, T. W., Gallippi, C. M., "Monitored Steady-State Excitation and Recovery (MSSER) Radiation Force Imaging Using Viscoelastic Models" *IEEE Transaction on Ultrasonics, Ferroelectrics, and Frequency Control*,Vol. 55, No. 7, 2008, pp. 1597-1610.

26. Pfeiler, T. W., Sumanasinghe, R. D., Loboa, E. G., "Finite element modeling of 3D human mesenchymal stem cell-seeded collagen matrices exposed to tensile strain." *Journal of Biomechanics* Vol. 41, 2008, pp. 2289-2296.

27.Lutz, H.T., Gharbi, H. A., Basics of Ultrasound. New York, NY. Spinger Berlin Heidelberg, 2006, pp1-19.

28. Greenleaf JF, Fatemi M, Insana M. Selected methods for imaging elastic properties of biological tissues. Annu Rev Biomed Eng 2003; 5:57–78.

29. Xydeas T, Siegmann K, Sinkus R, Krainick-Strobel U, Miller S, Claussen CD. Magnetic resonance elastography of the breast: correlation of signal intensity data with viscoelastic properties. Invest Radiol 2005; 40:412–420.

30. Glozman, T., Azhari, H., "A Method for Characterization of Tissue Elastic Properties Combining Ultrasound Computed Tomography With Elastography." J Ultrasound Med. Vol. 29 pp 387-398.

31. Nightingale, K., Soo, M. S., Nightingale, R., Trahey, G., "Acoustic Radiation Force Impulse Imaging: In Vivo Demonstration of Clinical Feasiblity." *Ultrasound in Medicine and Biology*. Oct 24, 2001

Chapter 3: Engineered Tissues and Their Biomechanical Properties

Background on Tissue Engineering

Integration of natural and synthetic materials to mimic native tissue structure and function is required for successful tissue engineering and replacement. Collagen has been extensively studied for its potential as a tissue engineering scaffold. It is the principle structural element of the extracellular matrix in most biological tissues with 90% of bone's organic matrix being comprised of collagen.[1]

Cells that supply specific function within the native tissue are crucial. Adult stem cells such as bone marrow derived mesenchymal stem cells (MSCs) have been extensively investigated for tissue engineering applications as they are easily accessible for autografting and exhibit multilineage differentiation capabilities.[2] Osteogenic differentiation in 3D culture is an essential step in creating bioengineered bone tissue. For differentiation to occur *in vitro* optimal mechanical and chemical stimuli are required.[3] MSCs cultured in the presence of ascorbic acid, β-glycerolphosphate, and

---

1. Knott L and Bailey AJ. "Collagen cross-links in mineralizing tissues: a review of their chemistry, function, and clinical relevance." *Bone*. Vol. 3, 1998, pp 181-187.
2. Taléns-Visconti, R., Bonora, A., Jover, R., Mirabet, V., Carbonell, F., Castell, J.V., and Gómez-Lechón, M.J., Hepatogenic differentiation of human mesenchymal stem cells from adipose tissue in comparison with bone marrow mesenchymal stem cells. *Shi Jie Wei Chang Bing Xue Za Zhi Ying Wen Ban.* 2006, Vol. *12*(36) pp. 5834.
3. Lacroix D., and Prendergast P.J., A mechano-regulation model for tissue differentiation during fracture healing: Analysis of gap size and loading. *J. Biomech.* Vol. 32, 1999, pp. 255.
4. Pittenger, M.F., Mackay, A.D., Beck, S.C., Jaiswal, R. F., Douglas, R., Mosca, J.D., Moorman, M.A., Simonetti, D.W., Craig, S., Marshak, D. R., "Multilineage Potential of Adult Human Mesenchymal Stem Cells." *Science* Vol. 284(5411) pp. 143-147.
5. Sottile V, Halleux C, Bassilana F, Keller H, Seuwen K. Stem cell characteristics of human trabecular bone-derived cells. *Bone* Vol. 30, 1999, pp 699-704
6. Halleux C, Sottile V, Gasser JA, Seuwen K. 2001. Multi-lineage potential of human mesenchymal stem cells following clonal expansion. *J Musculoskelet Neuronal Interact* 2: 71-76

dexamethasone have been shown to undergo osteogenic differentiation and deposit calcium [4, 5, 6]. Although cells grown within these conditions undergo differentiation *in vitro*, they lack the mechanical strength to withstand the *in vivo* environment. Therefore, it is important to produce cell constructs capable of withstanding the dynamic physiological stresses and strains within the *in vivo* environment[7].

It has also been shown MSCs are capable of osteogenic differentiation through mechanical stimulation of 10% and 12% strain.[8, 9, 10, 11]. During differentiation via mechanical stimulation, an increase in type 1 collagen and alkaline phosphatase was observed. In addition, upregulation of mRNA expression of bone morphogenic protein – 2 (BMP-2) was also detected.[12] A greater increase in BMP-2 has been noted in 10% strain over 12% strain.

Methods have been developed for applying a cyclic tensile strain to MSCs being grown for osteogenic differentiation. Special media constructs are designed to provide the optimum environment for cell growth and differentiation. The first step in creating the constructs involves seeding the cells within a linear 3D type 1 collagen matrix. Using TissueTrain (Flexcell® Hillsborough, NC) culture plates, the linear cell seeded collagen matrix is suspended between two anchors. By drawing a vacuum upon a plastic

---

7. Bonassar L.J., Vacanti C.A., "Tissue engineering: The first decade and beyond." *J Cell Biomchem* Vol. 30-31, 1998, pp297-303.

8. Hishikawa K, Miura S, Marumo T, et al. "Gene expression profile of human mesenchymal stem cells during osteogenesis in three-dimensional thermoreversible gelation polymer. " *Biochem Biophys Res Comm.* Vol. 317, 2004, pp. 1103-1107
9. Sumanasinghe RD, Bernacki SH, and Loboa EG. "Osteogenic differentiation of human mesenchymal stem cells in collagen matrices: effect of uniaxial cyclic tensile strain on bone morphogenetic protein (BMP-2) mRNA expression." *Tissue Eng*. Vol 12. 2006, pp.3459-3465.
10. Jaiswal, R. K., Jaiswal, N., Bruder, S. P., Mbalaviele, G.,Marshak, D. R., and Pittenger, M. F., "Adult human mesenchymal stem cell differentiation to the osteogenic or adipogenic lineage is regulated by mitogen-activated protein kinase." *J. Biol. Chem*. Vol. 275, 2000, pp. 9645.
11. Bruder, S. P., Jaiswal, N., and Haynesworth, S. E. "Growth kinetics, self-renewal, and the osteogenic potential of purified human mesenchymal stem cells during extensive subcultivation and following cryopreservation. *J. Cell Biochem*. Vol. 64, 1997 pp. 278.
12. Bell E, Ivarsson B, Merrill C. "Production of a tissue-like structure by contraction of collagen lattices by human fibroblasts of different proliferative potential in vitro." *Proc Natl Acad Sci USA*; Vol. 76, 1979, pp. 1274–1278
13. Pfeiler, T. W., Sumanasinghe, R. D., Loboa, E. G., "Finite element modeling of 3D human mesenchymal stem cell-seeded collagen matrices exposed to tensile strain." *Journal of Biomechanics* Vol. 41, 2008, pp. 2289-2296.

membrane in which the cell matrix rests, a tensile strain is applied.[13]

A limiting factor to successful production of tissue constructs is excessive contraction of collagen scaffolds which are observed during cell growth and differentiation. This contraction of the constructs presents an obstacle in that it limits the size of the final construct. Additional significant contraction by the cells causes rupture of the MSC-seeded collagen constructs when cyclic tensile strain is applied for more than two weeks. Understanding mechanical properties of MSC-seeded collagen gels and how those properties change during MSC proliferation and osteogenic differentiation will increase our understanding and use of these scaffolds for bone tissue engineering applications.[9, 14]

Biomechanical background of Biological Tissues and Mechanical Property Testing Methods.

Characterization of engineered tissues, other biological tissues, and even materials used in engineering applications require a calculation of "hardness" or the tendency of an object to deform under force application. A value used to describe this hardness is the elastic modulus. The elastic modulus is the tendency of an object to be deformed to be deformed elastically when a force is applied. Phenomenologially, this value is given as the slope of the stress-strain curve of an isotropic, elastic material. Therefore, the elastic modulus is defined as the stress (N/m^2) applied divided by strain (m/m). The equation for elastic modulus is

---

9. Sumanasinghe RD, Bernacki SH, and Loboa EG. "Osteogenic differentiation of human mesenchymal stem cells in collagen matrices: effect of uniaxial cyclic tensile strain on bone morphogenetic protein (BMP-2) mRNA expression." *Tissue Eng*. Vol 12. 2006, pp.3459-3465.

13. Pfeiler, T. W., Sumanasinghe, R. D., Loboa, E. G., "Finite element modeling of 3D human mesenchymal stem cell-seeded collagen matrices exposed to tensile strain." *Journal of Biomechanics* Vol. 41, 2008, pp. 2289-2296.

$$E = \frac{stress}{strain}$$

in which E(N/m^2) is equal to the elastic modulus. Stress is defined as the force applied per unit area and strain is calculated as the change in length (in direction force is applied) divided by the original length of the material.[15] The elastic modulus is useful in classifying the mechanical properties of materials, such as hardness, commonly used in engineering applications such as steel, iron, or copper.[16] One method for testing of the elastic modulus is use of a tensile test, which is the method used in testing tissue constructs. These machines work by using a hydraulic or electromagnetic machine that applies a force to the sample being tested. The tensile testing machine monitors the magnitude of the applied force along with the resulting strain due to the applied force. Ultimate tensile strength, peak stress, onset of permanent deformation and rupture can all be calculated by the machine. A stress strain curve is produced in which the slope of the linear portion of the curve is taken to be the Elastic modulus of the material tested. Both tensile (pulling) and compression (pushing) can be performed on samples tested for elastic modulus.[17] The elastic modulus is a very common value used in describing the hardness of materials since it is a value which is independent of shape or material dimensions.

Another value used to quantify stiffness of materials is the spring or stiffness constant, often referred to as "k". This value is mostly calculated using Hooke's Law of elasticity. Hooke's law is defined as:

---

15. Jiles, D., (2008). Introduction to the Principles of Materials Evaluation. CRC Press: New York, NY. Pp. 17-18.
16. Gedney, R,. "Tensile Testing Basics, Tips and Trends". *Quality Test and Inspection*. Admet Inc. January 2005.
17. "Young's Modulus (Elastic Modulus) – Strength (Mechanics) of Materials"*Engineers Edge"* Available (Online) http://www.engineersedge.com/material_science/youngs_modulus.htm. Accessed May 7, 2009.

$$F = -kx$$

in which F(N) is the force applied, k (N/m) is the spring constant, and x(m) is the displacement of the material from the point where no force is applied. Hooke's law was originally derived for characterizing elastic springs in which a linear relation existed between the compression or tension force applied to the spring and deformation from the equilibrium point. The calculation of the spring constant, k, can be calculated for any linearly elastic material, assuming the material behaves as an elastic spring. By Hooke's law, the value of the spring constant depends on both the elastic modulus and shear modulus of the material being tested.[18,19] The shear modulus of a material is the defined as the ratio of shear stress to shear strain.[20]

When characterizing the mechanical properties of biological materials, they are described as behaving as a viscoelastic material. Materials that exhibit viscoelastic properties are those which posses both viscous and elastic properties when being acted upon by a deforming force. Materials which exhibit elastic properties instantly strain when a force is applied and return to their initial state once the force is removed. Viscous materials show a resistance to shear flow and will result in a strain linearly with time when a force is applied. Materials which are viscoelastic have both of these properties and exhibit time dependent strain.[21]

In materials which are viscoelastic, the stress-strain relationship when plotted exhibits a curved shape (Figure 2). This is in contrast to materials which are linearly elastic and present a linear relationship between stress and strain (Figure 3).

---

18. Cowin, S. C., He, Q. C., (2005). "Tensile and Compresive Stress Yield Criteria for Cancellous Bone". *Journal of Biomechanics.* **38**:141-144
19. Mwanje, J., (1980). "An Approach to Hooke's Law." *Phys Educ.* **15**: 103-105.
20. Crandall, Dahl, Lardner (1959). *An Introduction to the Mechanics of Solids*. McGraw-Hill: New York
21. Meyer M. A., Chawla K.K., Mechanical Behavior of Materials. Prentice-Hall: Upper Saddle River, 1999, pp 98-103.

To better measure mechanical properties of viscoelastic materials, a step or constant force through time is used since strain is dependent upon time. This phenomenon in which stress is held constant while strain increases over time is referred to as creep In fact, mechanical property tests which use a constant force and then measure strain over time are referred to as creep tests. Another phenomena characteristic of viscoelastic materials, called relaxation, results in a decrease in stress as strain is held constant over time. In cases when a cyclic load is applied to a viscoelastic material, a phase lag can be observed. This lag in phase is due to the viscous nature which causes a dissipation of mechanical energy.[22]

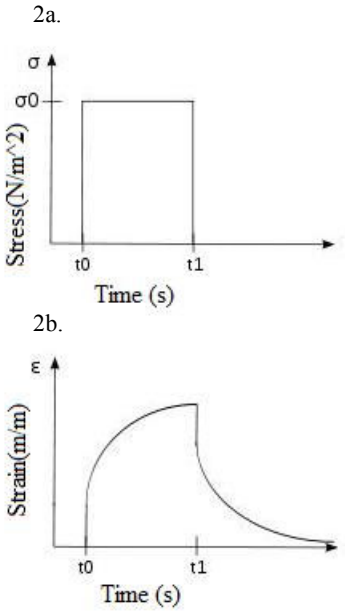

Figure 2a. Represents a constant stress applied over time to a viscoelastic material. Figure 2b. shows the change in strain over time even though constant force is applied to the viscoelastic material

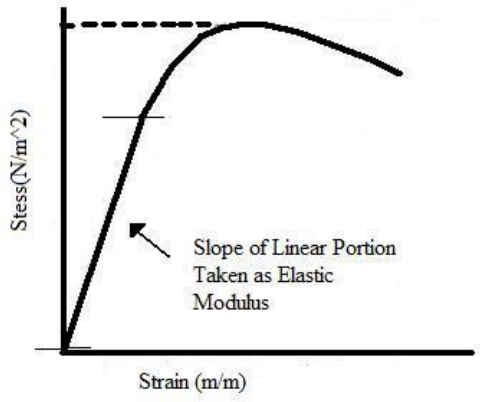

Figure 3. Shows response of a linearly elastic material when a deformation force is applied

22. Lakes,Roderic, Viscoelastic Materials, Cambridge University Press 2008 pp 1.5 New York, New York.

Mathematical models have been derived to characterize materials with viscoelastic properties. Some models include the Maxwell model, Kelvin-Voigt model and the Standard Linear Model. These are useful in predicting responses under loading conditions. Viscoelastic materials can be modeled using linear and parallel combinations of springs and dashpots each representing elastic and viscous properties respectively. Each model is different in the placement and number of these elements.[23] Depending on the stress versus strain relation, viscoelastic materials can be classified as having a linear or non-linear response. Materials which at low stresses behave as a rigid body, but act as a viscous fluid at high stresses are said to exhibit plastic deformation.[24]

Biomechanical properties of biological tissues are difficult to characterize due to a variety of reasons. Biological tissues are dependent upon time, moisture, and metabolically active with changes in properties after death.[25] Characterization and mathematical analysis requires the generalization of the behavior of biological materials. Mathematical models must be general enough to describe a wide variety of biological materials. Variations in temperature, boundary conditions, and sample size can affect the mechanical properties of biological materials. There is a limited amount of information that is available on the properties of soft tissues.

Biological materials which are mostly nonlinear and viscous often experience deformation and indention when acted upon by a stress. Such responses make biological materials very difficult to characterize due to this departure from following Hooke's law of elasticity for linear elastic materials. Models used to describe non-linear elastic materials use multiple

---

23. McCrum, N. G., "Principles of Polymer Engineering," Oxford University Press: 2003 pp. 117-122
24. Hosford, W. F., Mechanical Behavior of Materials Second Edition. Cambridge University Press: New York, NY. 2010. pp 20-33.
25. Krouskop, T. A., Wheeler, T. M., Kallel, F., Garra, B. S., Hall, T., (1998). "Elastic Moduli of Breast and Prostate Tissues Under Compression". *Ultrasonic Imaging.* **20**: 260-274.

parameters to characterize the elastic modulus. This results in multiple elastic modulus values. For biological materials which are not linearly elastic, indentation methods have been developed to better quantify the mechanical properties of such materials. These indentation methods, commonly used for calculation of the elastic moduli in biological materials, take into account the applied force, Poisson's Ratio, indentation depth, and indenter properties. Such methods have shown to be successful in calculating the Elastic moduli of some biological materials.[26,27] The biomechanical properties of biological tissue are being extensively studied due to changes that can occur during disease. A change in the stiffness of tissue is significant in that it occurs during many pathological processess.[28]

Haromonic Oscillator Model

Mathematical models have been derived for describing material response to an applied force. One such model that has been derived for such characterization is the harmonic oscillator model. The harmonic oscillator is a common mathematical model used in physics due to its wide range of application. The harmonic oscillation model consists of a spring with spring constant k (N/m) and a mass (kg) attached to one end while the other end of the spring is attached to a fixed point (Figure 4). When a displacing force is applied to the mass, the spring is either stretched or compressed from the equilibrium position. When this force is removed, the system experiences a restoring force equal and opposite to the applied force. This restorative force results in oscillation within the system. The restorative force depends

---

26. Samani A, Plewes D. (2004) "A method to measure the hyperelastic parameters of ex vivo breast tissuesamples." *Phys Med Biol*. **49**:4395–4405.
27. Puttini, S., et. al. (2009) "Gene-mediated Restoration of Normal Myofiber Elasticity in Dystrophic Muscles." *The American Society of Gene Therapy*. **17**: 19-25.
28. Erkamp, R.Q., Wiggins, P., Shovoroda, A.R., Emelianov, S.Y., and, O'Donnel, M., (1998). "Measuring the Elastic Modulus of Small Tissue Samples." *Ultrasonic Imaging* **20**: 17-28.

on the spring constant and the displacement of the mass from the equilibrium position. This restorative force is calculated through Hooke's law. A system in which the restorative force is the only force acting on the harmonic oscillator is referred to as a simple harmonic oscillator. In such systems, the mass follows a periodic oscillation motion with constant amplitude due to the restorative force. However, in a more realistic system damping, a decrease in amplitude, occurs which is caused by forces such as friction. This damping occurs as result in the loss of energy in the system. The loss of energy results in a decrease in amplitude through time.[29,30] Damped harmonic oscillators can be described by the following differential equation:

$$mx''+bx'+kx=0$$

In which m is mass constant, b the damping coefficient, and k the stiffness coefficient.

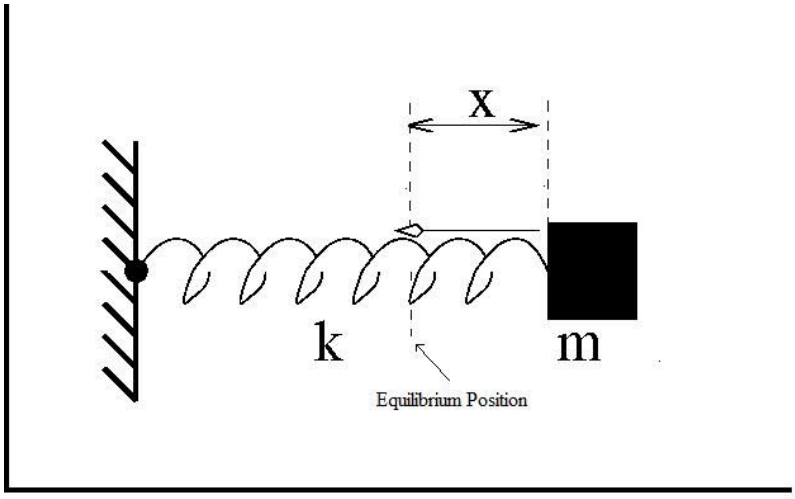

Figure 4 shows the arrangement of the harmonic oscillator model. A spring with stiffness constant k(N/m) is attached to a mass (kg) and attached to a fixed point. When a force is applied moving the mass out of the equilibrium position, a restorative force dependent upon x, the distance (m) of displacement from equilibrium and k moves the mass back to the equilibrium position.

29.O'Neil P. V., Advanced Engineering Mathematics 6th edition. Thompson: Toronto, Ontario. 2007. pp. 93-106.
30. Zill, D. G., Cullen, M. R., Differential Equations with Boundary-Value Problems. Brooks/Cole Publishing Company: New York, NY. Pp 170-182.

The damping coefficient will not be included in the calculation of elastic modulus. More details regarding this may be located in Chapter 4. When solving this differential equation of the harmonic oscillator, three different solutions for this model can be found dependent upon the determinant of the quadratic formula. These differences result in overdamped, critically damped, and underdamped solutions for the harmonic oscillator. (Figure 5) An overdamped solution gives an exponential decay back to the equilibrium position without any oscillation. This solution is a result of the determinant $b^2 - 4km > 0$. Such a solution results in two real roots from the characteristic equation giving decreasing exponential solutions for the differential equation. In fact, the Voigt model of viscoelasticity is derived from solutions of the overdamped oscillation model. The Voigt model extracts both the damping constant and spring constant from this model to use in the description of viscoelastic behavior. In a critically damped system, an exponential decay also occurs. Solving the differential equation for a critically damped system, using the characteristic equation, results in two equal real roots for the solution. Solving the differential equation for an underdamped system gives a much different solution as compared to the earlier two solutions. This is due to the determinant of $b^2 - 4km < 0$. The solution to such a differential equation gives two imaginary roots. This results in a solution which has terms of sines and cosines. Rather than having a solution which is a decreasing exponential, the solution is a damped, oscillating sine wave. The frequency of these oscillations may be calculated using parameters located within the differential equation for this model.[31,32] This equation for oscillation frequency is as

---

31.Choi, J. R., "Approach to the Quantum Evolution for Underdamped, Critically Damped, and Overdamped Driven Harmonic Oscillators Using Unitary Transformation." *Reports on Mathematical Physics* Vol. 52, 2003, pp. 321-329

32. Stephen T. Thornton and Jerry B. Marion, *Classical Dynamics of Particles and Systems, 5th Edition*, California: Thomson Books/Cole 2004

follows

$$f = \frac{1}{2\pi}\sqrt{\frac{k}{m}}$$

in which f equals the frequency of oscillation (Hz), k the stiffness constant (N/m) and m equals the mass constant (kg).[29]

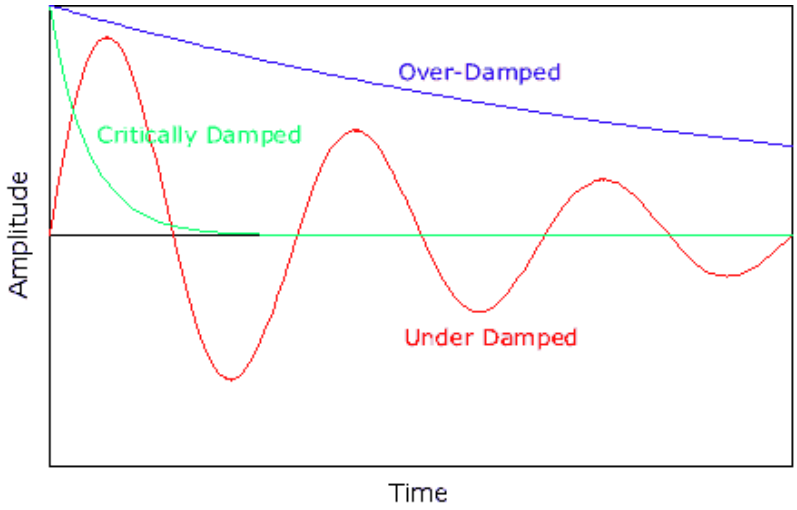

Figure 5 shows the three possible solutions for a damped harmonic oscillator. Overdamped and critically damped systems result in a decreasing exponential. Underdamped solutions give a solution which is a damped sine wave.[5]

Methods of Testing Mechanical Properties of Biological Materials

Although mechanical testing of biological materials is done using tensile tests, other methods have been developed in an attempt for a more accurate model. A method commonly used to measure the elastic modulus in biological materials is Atomic force microscopy (AFM). AFM was first invented in 1986 and is the most commonly used form of scanning probe microscope. It is a high-resolution scanning probe microscope that offers a resolution of fractions of a nanometer.

---

5. Sottile V, Halleux C, Bassilana F, Keller H, Seuwen K. Stem cell characteristics of human trabecular bone-derived cells. *Bone* Vol. 30, 1999, pp 699-704
29.O'Neil P. V., Advanced Engineering Mathematics 6th edition. Thompson: Toronto, Ontario. 2007. pp. 93-106.

AFM is utilized extensively for imaging, measuring, and manipulation at the nanoscale level. The AFM consists of a cantilever made typically from silicon or silicon nitride with a sharp tip or probe fixed to the very end of the cantilever. AFM was originally invented for use in imaging nanometer sized organic and biological materials. AFM instruments come available with a force curve mode that will record up and down deflections of the cantilever beam. It is this mode this has been used in indentation studies for determining of mechanical properties such as Elastic modulus.[37] AFM has been used to measure mechanical properties of cells and adhesive forces between them. These properties are measured with the micrometer-scale cantilever by applying a stress to the surface. Once the cantilever makes contact, continued force results in a deflection. The resulting deflection or strain can be measured in a couple different ways.[38] Most AFMs use a laser beam system for detecting the deflection of the cantilever arm. In such systems, a laser is used to monitor the deflection of the beam. Another method used is fitting a strain gauge to the cantilever. Using a Wheatstone bridge, the deflection of the cantilever may be measured. Proper functioning of the AFM relies on the forces between the tip and sample. The deflection of the cantilever is dependent upon and obeys Hooke's law of elasticity. Hooke's law is used to properly calculate the forces and deflection used in this system. The force applied to the surface from the cantilever is kept constant while k, the stiffness, is a constant specific to the cantilever material. The value of x changes as the cantilever is moved over the sample. This change in x is a result in elevation and stiffness differences along the sample.[39]

---

37. A. D. L. Humphris, M. J. Miles, and J. K. Hobbs. (2005) A Mechanical Microscope: High-speed Atomic Force Microscopy. *University of Bristol, H.H. Wills Physics Laboratory Applied Physics Letters* **86**: 034106
38. Chaudhuri, O., Parekh, S., Lam, W., Fletcher, D., "Combined Atomic Force Microscopy and Side-Vew Optical Imaging for Mechanical Studies of Cells." *Nature Methods* Vol 6. No. 5, May 2009.
39. "Atomic Force Microscopy" *nanoScience Instruments*. Available (Online) http://www.nanoscience.com/education/AFM.html. Accessed May 5, 2009.

Since biological materials are not linearly elastic and often experience deformation and indention, other mathematic models must be applied to indention studies in determining the Elastic modulus. One such model is the Sneddon model which uses force and a measure of the indentation by the tip into the material to calculate the Elastic modulus of the material.

The Sneddon model of indentation is commonly used to predict the Elastic modulus in biological materials. This model takes into account the relationship between indenter shape (indenter connected to cantilever) and the resulting indentation depth due to the force applied. The vertical force, indentation depth and Elastic modulus can be related through a series of equations. Three such equations, for a cylindrical indenter, conical indenter, and a parabolic indenter are as follows:

Cylindrical:

$$F = \frac{2EaI}{(1-v^2)}$$

Conical:

$$F = \frac{2E\tan\theta}{\pi(1-v^2)} I^2$$

Parabolic:

$$F = \frac{4E}{3(1-v^2)}(RI^3)^{1/2}$$

Where F (N/m^2) is equal to the vertical force, E(N/m^2) is the Elastic modulus, a(m) is the radius of the cylindrical indenter, I(m) is depth of indentation, v is Poisson's Ratio, θ is the angle opening of the cone, and R(m) is he effective tip radius. If AFM tip is pyramidal, then an approximation by using either cylindrical or cone may be used[40]. This model, designed for macroscopic applications, has also been used in microscopic ones as well. The Sneddon model assumes the sample has an infinitely wide surface that is flat in the x and y coordinate and the sample is infinitely thick. For thin samples in which the effect of the substrate beneath the sample may not be neglected, the effect of the substrate must be accounted for.[41]

Strengths and Shortcomings of Current Mechanical Property Testing Methods in Engineered Tissues

Methods have already been development to measure and quantify the elastic properties of cell-seeded collagen gel matrices cultured under cyclic tensile strain. Previous work used Finite Element Analysis (FEA) to predict local stresses and strains within these constructs. The FEA models were assembled using construct geometry (i.e. construct dimensions) and material property data experimentally obtained. Material data property was obtained using a tensile testing machine under ramp displacement control. The Elastic modulus was calculated by averaging stiffness values. These values were

---

40. Ikai, A., Afrin, R., (2003) Toward Mechanical Manipulations of Cell Membranes and Membrane Proteins Using an Atomic Force Microscopy. *Cell Biochemistry and Biophysics*. **39**: 257-277
41. Puttini, S., et. al. (2009) "Gene-mediated Restoration of Normal Myofiber Elasticity in Dystrophic Muscles." *The American Society of Gene Therapy*. **17**: 19-25.

taken from the linear portion of the stress-strain relation. Performing a tensile test requires the removal of constructs from tissue media, stretching of constructs (up to 150% strain), and ultimate destruction of the tissue constructs.[42]

Current methods are highly invasive resulting in death of the cells and ultimate destruction of the tissue constructs. This is not only a waste of money and resources, but also time invested in creating these tissue constructs. In addition to being highly invasive, the tensile test the properties of the tissue construct as a whole and does not provide specific information about local differences which may exist within the construct. The FEA is performed using geometric parameters of the tissue constructs and the results of the tensile tests. However, there are issues with the accuracy of the FEA model. For the purpose of modeling, the tissue constructs are assumed be linearly elastic, which is not true of viscoelestic materials. These materials experience strain that is dependent upon time and not solely upon magnitude of force application. However, FEA allows for reporting of three dimensional data. Strain information is given for the tissue constructs in the axial, elevational, and lateral directions whereas MSSER provides only two dimensional information.

Issues also exist with using AFM in testing the mechanical properties. In order for measurements to occur, the cantilever arm must come in contact with the tissue constructs rendering it an invasive technique. Another issue inherit with AFM is the presence of intermolecular forces between the tissue construct and the cantilever arm. These intermolecular forces could result in inaccuracies in measurements.[43] Ultrasound methods

---

42. Pfeiler, T. W., Sumanasinghe, R. D., Loboa, E. G., "Finite element modeling of 3D human mesenchymal stem cell-seeded collagen matrices exposed to tensile strain." *Journal of Biomechanics* Vol. 41, 2008, pp. 2289-2296.
43. (old 2.) Chaudhuri, O., Parekh, S., Lam, W., Fletcher, D., "Combined Atomic Force Microscopy and Side-Vew Optical Imaging for Mechanical Studies of Cells." *Nature Methods* Vol 6. No. 5, May 2009.

provide an additional benefit in that it is an internal method of force application, applying the compression force to all depths within the tissue construct and measuring change in displacement at all depths. However, AFM is an external method of force application in which the force is applied externally to the top surface and only one measurement of displacement, at the surface, is obtained. An advantage AFM does provide over MSSER the much higher resolution capability. AFM resolution is on the order of nanometers while MSSER resolution is on the order or several hundred microns. AFM also has much higher sensitivity; it is capable of measuring displacements of less than a nanometer, much smaller than what of which MSSER is capable.

MSSER vs. Current Methods and the Need for Better Methods

MSSER imaging of tissue constructs holds the possibility of being able to determine the mechanical properties of tissue constructs while they are alive and growing in culture media. MSSER is also non-invasive and allows for internal force application and internal measurements of displacements. This technology could allow for monitoring of changes in mechanical properties of tissue constructs throughout the differentiation process. MSSER along with viscoelastic models provide for a more accurate model to characterize the mechanical properties of the cells. FEA models assume a linear elastic relationship between stress and strain, but MSSER, produced to mimic a creep test, can report changes in strain over time during constant force application. This new MSSER technique, in contrast to earlier methods, allows for measuring of localized stiffness values within the construct. This

is extremely helpful in that it will allow for detection of areas along the construct that are stiffer than others. This can be used to determine areas in which differentiation is occurring or points of higher stress within the construct. It is possible to detect areas in which calcium has been deposited within the differentiating constructs. MSSER does not have as high of a resolution as other techniques. Current MSSER imaging systems only have a resolution of several hundred microns. Therefore, it would be difficult to discern differences in elastic modulus on a scale smaller than a few hundred microns. In the current setup of MSSER, only one elevational position is imaged, thus elastic modulus differences in the elevational direction are not reported. In addition, it would be very difficult to obtain information in the elevational direction due to the thin size of the tissue construct and poor resolution.

Applying MSSER to Test the Mechanical Properties of Engineered Tissue Being Grown for Osteogenic Differentiation

MSSER in past work was used in conjunction with the Voigt model of elasticity to calculate the Elastic modulus along with other mechanical property parameters.[44] However, these tissue constructs present a unique challenge in that they are very thin and resemble a rope suspended between to anchors. Imaging of these constructs is quite different from imaging a large section of tissue. After unsuccessfully trying to use the Voigt model of elasticity to characterize these constructs, others models were explored. The Voigt model gave incorrect tissue recovery values which resulted in model curves that did not fit the

---

44. Mauldin, F. W. Jr., Haider, M. A., Loboa, E. G., Behler, R. H., Euliss, L. E., Pfeiler, T. W., Gallippi, C. M., "Monitored Steady-State Excitation and Recovery (MSSER) Radiation Force Imaging Using Viscoelastic Models" *IEEE Transaction on Ultrasonics, Ferroelectrics, and Frequency Control*,Vol. 55, No. 7, 2008, pp. 1597-1610.

actual displacement models. It was determined the reason for these errors was data better modeled an underdamped harmonic oscillator rather than an overdamped harmonic oscillator from which the Voigt model of elasticity was derived. The underdamped harmonic oscillator provided for a more accurate model to describe the behavior of these constructs, specifically the oscillation which occurs after cessations of the excitation force. This underdamped harmonic oscillation model was used to calculate a spring constant which describes the stiffness. Using MSSER parameters, underdamped harmonic oscillation model, along with some components of the Voigt model, methods were developed to calculate the Elastic modulus of these tissue constructs.

Conclusion

Tissue engineering for the purpose of bone replacement therapy relies on integration of natural and synthetic components. For osteogenic differentiation to occur, specific chemical and mechanical stimulation is required. For these bone tissue constructs to ever be successfully used in bone replacement therapies, much more work is needed to better changes in size and increase in hardness, due to calcium deposition, during differentiation. Mechanical properties of biological materials are difficult to characterize due to their viscoelastic nature. Methods have been developed in an attempt to better characterize biological materials even though most methods assume these materials are linearly elastic. Novel ultrasonic imaging methods, MSSER, have also been developed in attempt to provide a more accurate and non-invasive method of testing the mechanical properties of viscoelastic biological materials. Hopes are to develop MSSER into a non-invasive mechanical property testing method used to determine the elastic modulus of tissue constructs providing localized stiffness values for specific areas along the construct.

1. Knott L and Bailey AJ. "Collagen cross-links in mineralizing tissues: a review of their chemistry, function, and clinical relevance." *Bone*. Vol. 3, 1998, pp 181-187.

2.Taléns-Visconti, R., Bonora, A., Jover, R., Mirabet, V., Carbonell, F., Castell, J.V., and Gómez-Lechón, M.J., Hepatogenic differentiation of human mesenchymal stem cells from adipose tissue in comparison with bone marrow mesenchymal stem cells. *Shi Jie Wei Chang Bing Xue Za Zhi Ying Wen Ban.* 2006, Vol. *12*(36) pp. 5834.

3. Lacroix D., and Prendergast P.J., A mechano-regulation model for tissue differentiation during fracture healing: Analysis of gap size and loading. *J. Biomech.* Vol. 32, 1999, pp. 255.

4. Pittenger, M.F., Mackay, A.D., Beck, S.C., Jaiswal, R. F., Douglas, R., Mosca, J.D., Moorman, M.A., Simonetti, D.W., Craig, S., Marshak, D. R., "Multilineage Potential of Adult Human Mesenchymal Stem Cells." *Science* Vol. 284(5411) pp. 143-147.

5. Sottile V, Halleux C, Bassilana F, Keller H, Seuwen K. Stem cell characteristics of human trabecular bone-derived cells. *Bone* Vol. 30, 1999, pp 699-704

6. Halleux C, Sottile V, Gasser JA, Seuwen K. 2001. Multi-lineage potential of human mesenchymal stem cells following clonal expansion. *J Musculoskelet Neuronal Interact* 2: 71-76

7. Bonassar L.J., Vacanti C.A., "Tissue engineering: The first decade and beyond." *J Cell Biomchem* Vol. 30-31, 1998, pp297-303.

8. Hishikawa K, Miura S, Marumo T, et al. "Gene expression profile of human mesenchymal stem cells during osteogenesis in three-dimensional thermoreversible gelation polymer. " *Biochem Biophys Res Comm.* Vol. 317, 2004, pp. 1103-1107

9. Sumanasinghe RD, Bernacki SH, and Loboa EG. "Osteogenic differentiation of human mesenchymal stem cells in collagen matrices: effect of uniaxial cyclic tensile strain on bone morphogenetic protein (BMP-2) mRNA expression." *Tissue Eng*. Vol 12. 2006, pp.3459-3465.

10. Jaiswal, R. K., Jaiswal, N., Bruder, S. P., Mbalaviele, G.,Marshak, D. R., and Pittenger, M. F., "Adult human mesenchymal stem cell differentiation to the osteogenic or adipogenic lineage is regulated by mitogen-activated protein kinase." *J. Biol. Chem*. Vol. 275, 2000, pp. 9645.

11. Bruder, S. P., Jaiswal, N., and Haynesworth, S. E. "Growth kinetics, self-renewal, and the osteogenic potential of purified human mesenchymal stem cells during extensive subcultivation and following cryopreservation. *J. Cell Biochem*. Vol. 64, 1997 pp. 278.

12. Bell E, Ivarsson B, Merrill C. "Production of a tissue-like structure by contraction of collagen lattices by human fibroblasts of different proliferative potential in vitro." *Proc Natl Acad Sci USA*; Vol. 76, 1979, pp. 1274–1278.

13. Pfeiler, T. W., Sumanasinghe, R. D., Loboa, E. G., "Finite element modeling of 3D human mesenchymal stem cell-seeded collagen matrices exposed to tensile strain." *Journal of Biomechanics* Vol. 41, 2008, pp. 2289-2296.

14. Sumanasinghe RD, Osborne JA, Loboa EG. "Mesenchymal stem cell-seeded collagen matrices for bone repair: effects of cyclic tensile strain, cell density, and media conditions on matrix contraction in vitro." *J Biomed Mater Res A.* Vol. 88(3), 2009. pp. 778-86.

15. Jiles, D., (2008). Introduction to the Principles of Materials Evaluation. CRC Press: New York, NY. Pp. 17-18.

16. Gedney, R,. "Tensile Testing Basics, Tips and Trends". *Quality Test and Inspection*. Admet Inc. January 2005.

17. "Young's Modulus (Elastic Modulus) – Strength (Mechanics) of Materials"*Engineers Edge"* Available (Online) http://www.engineersedge.com/material_science/youngs_modulus.htm. Accessed May 7, 2009.

18. Cowin, S. C., He, Q. C., (2005). "Tensile and Compresive Stress Yield Criteria for Cancellous Bone". *Journal of Biomechanics.* **38**:141-144

19. Mwanje, J., (1980). "An Approach to Hooke's Law." *Phys Educ.* **15**: 103-105.

20. Crandall, Dahl, Lardner (1959). *An Introduction to the Mechanics of Solids*. McGraw-Hill: New York

21**.** Meyer M. A., Chawla K.K., Mechanical Behavior of Materials. Prentice-Hall: Upper Saddle River, 1999, pp 98-103.

22. Lakes,Roderic, Viscoelastic Materials, Cambridge University Press 2008 pp 1.5
New York, New York.

23. McCrum, N. G., "Principles of Polymer Engineering," Oxford University Press: 2003 pp. 117-122

24. Hosford, W. F., Mechanical Behavior of Materials Second Edition. Cambridge University Press: New York, NY. 2010. pp 20-33.

25. Krouskop, T. A., Wheeler, T. M., Kallel, F., Garra, B. S., Hall, T., (1998). "Elastic Moduli of Breast and Prostate Tissues Under Compression". *Ultrasonic Imaging.* **20**: 260-274.

26. Samani A, Plewes D. (2004) "A method to measure the hyperelastic parameters of ex vivo breast tissue samples." *Phys Med Biol*. **49**:4395–4405.

27. Puttini, S., et. al. (2009) "Gene-mediated Restoration of Normal Myofiber Elasticity in Dystrophic Muscles." *The American Society of Gene Therapy*. **17**: 19-25.

28. Erkamp, R.Q., Wiggins, P., Shovoroda, A.R., Emelianov, S.Y., and, O'Donnel, M., (1998). "Measuring the Elastic Modulus of Small Tissue Samples." *Ultrasonic Imaging* **20**: 17-28.

29.O'Neil P. V., Advanced Engineering Mathematics 6th edition. Thompson: Toronto, Ontario. 2007. pp. 93-106.

30. Zill, D. G., Cullen, M. R., Differential Equations with Boundary-Value Problems. Brooks/Cole Publishing Company: New York, NY. Pp 170-182.

31.Choi, J. R., "Approach to the Quantum Evolution for Underdamped, Critically Damped, and Overdamped Driven Harmonic Oscillators Using Unitary Transformation." *Reports on Mathematical Physics* Vol. 52, 2003, pp. 321-329

32. Stephen T. Thornton and Jerry B. Marion, *Classical Dynamics of Particles and Systems, 5th Edition*, California: Thomson Books/Cole 2004

33. Splung Physics.com "Damped Oscillations" Available (Online)
http://www.splung.com/content/sid/2/page/damped_oscillations. Accessed March 12, 2010.

34.Singh, B. N., Tahtinen, S., Moilanen., Jacquet, P., Dekeyser, J., (2003). "In-reactor Uniaxial Tensile Testing of Pure Copper at a Constant Strain rate at 90˚C." *Journal of Nuclear Materials.* **320**: 299-304.

35. Momoh, J. J., Ajueyitsi, O.A., Onipede, A. M., (2008). "Development of a Low Cost Mechanically Operated Tensile and Creep Testing Machine." *Journal of Engineering and Applied Sciences*. **6**: 491-495.

36. Lynnworth, L. C., E. P. Papadakis, K. A. Fowler, (1977) "Ultrasound Propagation Measurements and Applications," *International Advances in Nondestructive Testing*. **5**: 71-115.

37. A. D. L. Humphris, M. J. Miles, and J. K. Hobbs. (2005) A Mechanical Microscope: High-speed Atomic Force Microscopy. *University of Bristol, H.H. Wills Physics Laboratory Applied Physics Letters* **86**: 034106

38. Chaudhuri, O., Parekh, S., Lam, W., Fletcher, D., "Combined Atomic Force Microscopy and Side-Vew Optical Imaging for Mechanical Studies of Cells." *Nature Methods* Vol 6. No. 5, May 2009.

39. "Atomic Force Microscopy" *nanoScience Instruments*. Available (Online)
http://www.nanoscience.com/education/AFM.html. Accessed May 5, 2009.

40. Ikai, A., Afrin, R., (2003) Toward Mechanical Manipulations of Cell Membranes and Membrane Proteins Using an Atomic Force Microscopy. *Cell Biochemistry and Biophysics*. **39**: 257-277

41. Puttini, S., et. al. (2009) "Gene-mediated Restoration of Normal Myofiber Elasticity in Dystrophic Muscles." *The American Society of Gene Therapy*. **17**: 19-25.

42. Pfeiler, T. W., Sumanasinghe, R. D., Loboa, E. G., "Finite element modeling of 3D human mesenchymal stem cell-seeded collagen matrices exposed to tensile strain." *Journal of Biomechanics* Vol. 41, 2008, pp. 2289-2296.

43. (old 2.) Chaudhuri, O., Parekh, S., Lam, W., Fletcher, D., "Combined Atomic Force Microscopy and Side-Vew Optical Imaging for Mechanical Studies of Cells." *Nature Methods* Vol 6. No. 5, May 2009.

44. Mauldin, F. W. Jr., Haider, M. A., Loboa, E. G., Behler, R. H., Euliss, L. E., Pfeiler, T. W., Gallippi, C. M., "Monitored Steady-State Excitation and Recovery (MSSER) Radiation Force Imaging Using Viscoelastic Models" *IEEE Transaction on Ultrasonics, Ferroelectrics, and Frequency Control*,Vol. 55, No. 7, 2008, pp. 1597-1610.

Chapter 4: MSSER Imaging of Tissue Constructions Grown in Complete Growth Media versus Osteogenic Media

Methods

Cell isolation and culture.

Human Mensenchymal Stem Cells (MSCs) were isolated from trabecular bone fragments of a 78 year old female donor.[1] Briefly, dissected bones were digested with collagenase XI (3 mg/mL) in phosphate buffered saline (PBS) at 37^{o}C for three hours on a rotator plate (Labquake, rotisserie mode). After three hours, complete growth medium (α-MEM supplemented with 10% fetal bovine serum (FBS, lot selected; Atlanta Biologicals, Lawrenceville, GA), 2 mM L-glutamine, 100 units/mL penicillin, and 100 μg/mL streptomycin) was added to the digest to neutralize the collagenase. Debris was removed by filtering the digest through a 100 μm cell strainer followed by centrifugation at 500 g for 5 minutes. The pellet was resuspended in 160 mM NH_4Cl for 10 minutes, centrifuged to remove the supernatant, and the cells plated in complete growth medium. Non-adherent cells were washed out after 24 hours. Passage 2 hMSCs were used for all experiments and analyses.

---

1. Bernacki SH, Wall ME, and Loboa EG. 2008. Isolation of human mesenchymal stem cells from bone and adipose tissue. Methods Cell Biol.;86:257-78.
2. Sumanasinghe RD, Bernacki SH, and Loboa EG. 2006. Osteogenic differentiation of human mesenchymal stem cells in collagen matrices: effect of uniaxial cyclic tensile strain on bone morphogenetic protein (BMP-2) mRNA expression. Tissue Eng. Dec;12(12):3459-65.

Fabrication of collagen gels.

Linear three-dimensional MSC-seeded constructs were fabricated as previously described in Sumanasinghe et al.[2] Briefly, MSCs were seeded into collagen gels at 60,000 cells/ 200 μl/ construct. Gel solution consisted of 70% type I collagen (BD Biosciences, San Jose, CA) (pH adjusted to 7.0), 20% 5x MEM and 10% FBS. The hMSC-seeded collagen gel solutions were loaded into Tissue Train™ collagen I-coated six-well culture plates (Flexcell International, Hillsborough, NC) and were allowed to polymerize for 2 hours prior to application of growth media.

Osteogenic differentiation

Beginning 24 hours after seeding with MSCs, the constructs were cultured for an additional two weeks in either growth or osteogenic media. Osteogenic medium consisted of growth medium supplemented with 50 μM ascorbic acid, 0.1 μM dexamethasone, and 10 mM β-glycerolphosphate. Tissue cell constructs were prepared by Audrey Charoenpanich in the Loboa lab at North Carolina State University.

Creation of sequences

In order to perform Monitored Steady State Excitation and Recovery (MSSER), ultrasound beam sequences were created for use in imaging of cell constructs. The designed MSSER sequence utilized 2 different types of beams which included a high intensity 10 cycle pushing beam and a conventional 2 cycle B-mode tracking pulse. The MSSER sequence began with two B-mode pulses which were used to determine an initial reference point. After firing of the two tracking pulses, 40 high intensity, 10 cycle ARFI pushing beams were used to displace the tissue. After each of the 40 high intensity pushing pulses, a B-mode tracking pulse was used to monitor the displacement during force excitation. This alternation between pushing and tracking pulses was desirable in order to mimic a creep test;

applying a constant force while monitoring changes in strain over time. Following this push and track sequence, an additional 1999 tracking pulses were used to track the recovery of tissue and monitor the oscillation frequency of the tissue constructs. Imaging was performed using an F/#1.5 focal configuration. Using a linear array clinical ultrasound transducer, ultrasound waves were focused to one lateral position. The imaging sequence was designed this way in order to eliminate undesired vibrations within the construct which could interfere with measurements. Shear waves, generated by pushing over multiple areas, were found in previous experiments to travel within the construct and interfere with proper data acquisition. Although a shear wave was still created from pushing and tracking in one location, it only appeared to interfere with oscillation data. Therefore, phase slope filtering was performed to remove shear wave interference. In addition, a high pass filter was also used to remove low frequency data within the tissue

A pulse repetition frequency of 7.39 kHz was used for both pushing and tracking beams. Pushing beams were administered with a frequency of 4.21MHz and tracking beams with a 6.15MHz frequency. The entire duration of the force excitation was 10.8 ms while the following tracking sequences were 270.5ms in duration. The entire imaging sequence was 281.3 ms in duration.

Preparation of Cell Imaging Bath

In preparation for imaging of cells, a Phosphate Buffer Solution (PBS) was prepared. Solution was prepared using 8 grams of sodium chloride, 0.2 grams potassium chloride, 1.44 grams of sodium phosphate, and 0.24 grams of potassium phosphate per liter of deionized water. Approximate 12 liters of solution were prepared. A Sterilite® plastic container was used to contain PBS, This container was placed into a Stable-Temp® (Cole-Parmer, Vernon

Hills, IL) water bath heater and heated to a temperature of 37 degrees Celsius. This bath temperature was maintained throughout the duration of cell construct imaging. Cells were kept as close to 37 degrees Celsius as possible from the time they were removed from the incubator until imaging was completed.

Imaging of Cells

Imaging of tissue constructs were performed using a Siemens SONOLINE Antares ultrasound scanner (Siemens Medical Solutions USA, Inc.,) using a VF7-3 linear array transducer. Tissue constructs were imaged at day 14. In preparation for imaging, these tissue constructs were first removed from the incubator and then using a pipette, culture media was removed. Plastic membranes were also removed from all cell culture plates ensuring cell constructs were left intact suspended between anchors. These steps were done quickly in order to ensure cells would be alive while imaged. After removal of membranes, tissue construct plates were submerged into PBS bath and suspended in this bath using ring stand rods. Using a motion translation stage, in which the ultrasound transducer was placed, along with Labview®, precise movement of the transducer along the length of the construct for imaging was ensured. This incremental imaging was required since the ultrasound beam was focused to only one lateral position. Movement of the transducer along the tissue construct was incremented at .5mm per step. The lateral field of view for each imaging point was .535 mm. Approximately 21-22 images were acquired across each construct. This resulted in approximately an 11mm length of each construct being imaged. Labview® was used to acquire the image, move the transducer the desired incremental length, and then wait one minute before the next image was acquired to allow for any shear or oscillation waves in the tissue constructs to cease. Collected radio frequency (RF) data was processed into axial

ARFI-induced displacements using one-dimensional cross correlation. The search regions were set to a length of 0.66mm with a kernel of length 0.54mm.

Fitting MSSER data to Harmonic Oscillation Model and Calculation of Elastic Modulus

Processing of data

During the imaging process, three tissue constructs grown in osteogenic differentiation media and two tissue constructs grown in complete growth media were imaged. Processed RF data provided strain information for the tissue construct during force excitation along with tissue recovery information and oscillation frequency of the tissue constructs at force cessation. For each point in the imaging field, at a given lateral and axial location in the image, an ARFI data curve with displacement information throughout the imaging period was produced. ARFI data curves were filtered based on excitation data. These curves were kept on the basis of how well the excitation data fit an increasing exponential. Filtering of data was performed in two different ways to provide two different data sets. The first set included data filtered using a low R^2 value of 0.8 and then using a higher R^2 value of 0.95. A third data set was also produced in which all curves were kept regardless of how well excitation data fit an increasing exponential. Curves were filtered in order to remove noisy data points. An increasing exponential was chosen since this model best describes the response of viscoelastic materials under constant force.

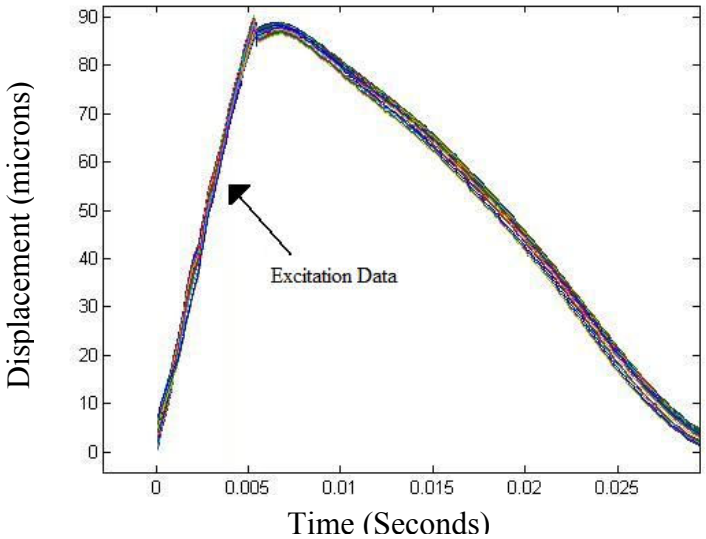

Selected Curves using an Increasing Exponential Fit and R^2 Value of 0.95.

Harmonic Oscillation Model

Since the recovery data from these tissue constructs follows the underdamped solution of the harmonic oscillator, this model can be used to predict the spring constant of these tissue constructs. For the purpose of calculating the elastic modulus, the data from each curve was divided into two separate regions; the excitation data which fit an increasing exponential typical of viscoelastic materials, and the recovery data which followed the underdamped harmonic oscillation model. For purposes of fitting to the model, the recovery and oscillation data was assumed to follow the underdamped response of a harmonic oscillation with a mass being displaced an initial amount then released and allowed to oscillate.

From using excitation and oscillation data, spring constant values were calculated using a formula for the oscillation frequency of a harmonic oscillator. This frequency is calculated using the mass constant and spring constant. This formula solved for the spring constant is as follows

$$k = (2\pi f)^2 m$$

where f (seconds) is the oscillation frequency of the construct, k (N/m) the spring constant and m(kg) is the mass constant.

Calculation of Oscillation Frequency

To determine the oscillation frequency of each curve in the data, a Fourier Transform was performed on all curves that were selected during filtering. A high pass filter was applied to the frequency data removing noisy low frequency data. The oscillation frequency, calculated from high pass filtered Fourier transform data, was taken as the highest frequency peak. These frequency data were saved to be used in the calculation for the elastic modulus

Calculation of Mass Constant

In order to calculate the spring constant, the mass constant of each curve had to be calculated. This mass constant was calculated using Newton's 2nd law, solving for mass in which

$$m = \frac{F}{A}$$

where m is equal to the mass(kg), F is equal to Force(N) and A is equal to the acceleration of the tissue(N/m^2). The force used in this calculation is the acoustic radiation force magnitude. This value is obtained by first calculating the ultrasonic body force given by

$$\left|\vec{F}\right| = \frac{Wabsorbed}{c} = \frac{2\alpha I}{c}$$

In which $\left|\vec{F}\right|$ (N/m^3) is the body force, α (Np/m) is the absorption coefficient of the media, I (W/m^2) is the temporal average intensity and c(m/s) is the speed of sound. In this calculation, c was set equal to 1497m/s which is the approximate speed of sound through the PBS

medium in which imaging was performed. Alpha was set equal to 24.23 Np/m, which is the attenuation coefficient of biological materials. The temporal average intensity, I, was set equal to 1114W/cm^2. To get force magnitude, the body force was multiplied by the lateral, elevational, and axial resolutions. This relation is given by

$$F = \left|\vec{F}\right| * l_{lat} * l_{elev} * l_{axial}$$

where F(N) is the force magnitude, $\left|\vec{F}\right|$ is the body force (N/m^3) l_{lat} (m) is the lateral resolution, l_{elev} (m) is the elevational resolution, and l_{axial} (m) is the axial resolution. The resolutions were 535 microns, 600 microns, and 600 microns respectively.

Two different methods were used in calculating the acceleration of the tissue during force excitation. The first method fit an increasing exponential curve to the excitation data. This model was chosen since it best describes the change in strain of viscoelatic biological materials under constant stress. Once this position curve was calculated, the second derivate was calculated to give an equation for acceleration of the tissue construct during excitation. The position curve was in the form of

$$a - a * e^{-\frac{x}{b}}$$

while the acceleration curve was in the form

$$-\frac{a}{b^2} * e^{-\frac{x}{b}}$$

An average acceleration was calculated by first calculating the acceleration at each point throughout the excitation period using the acceleration equation. These accelerations were then averaged together and used as an average acceleration for the tissue.

In an attempt to generate an average acceleration value which was not time dependent, a 2nd order polynomial fit to excitation data was also performed. This excitation data was fit to a second order polynomial in the form

$$Ax^2+Bx+C$$

The second derivative was calculated from this estimated polynomial giving an acceleration value for the tissue construct during excitation. Use of both of these methods resulted in an additional two different data sets.

Calculation of the Elastic Modulus

Using the underdamped harmonic oscillation model, it is possible to calculate the spring constant of these tissue constructs. It is from this value the elastic modulus may be calculated. Using formulas taken from previous work (Mauldin et. al.) and formulas for calculating the elastic modulus, this modulus value may be calculated.[3] It is first assumed this spring constant k(N/m) is equal to the relaxed elastic modulus E_u (N/m) of the tissue constructs.

$$k = E_u$$

---

3. Mauldin, F. W. Jr., Haider, M. A., Loboa, E. G., Behler, R. H., Euliss, L. E., Pfeiler, T. W., Gallippi, C. M., "Monitored Steady-State Excitation and Recovery (MSSER) Radiation Force Imaging Using Viscoelastic Models" *IEEE Transaction on Ultrasonics, Ferroelectrics, and Frequency Control*,Vol. 55, No. 7, 2008, pp. 1597-1610.

The following relation has been shown between the force magnitude A (N), the relaxed elastic modulus E_u (N/m), and the strain (m).

$$Eu = \frac{A}{X_{ss}} = \frac{\left|\vec{F}\right|(l_{axial} * l_{elev} * l_{lat})}{X_{ss}}$$

In these formulas, X_{ss} is equal to the steady state displacement, $\left|\vec{F}\right|$ the ultrasonic acoustic body force, l_{axial} the axial resolution, l_{elev} the elevational resolution, and l_{lat} the lateral resolution with all of these in units of meters. The elastic modulus (N/m^2) is given by a similar relation where

$$E = \frac{\left|\vec{F}\right|(l_{elev} * l_{lat})}{X_{ss}}$$

in which E(N/m2) is the elastic modulus, $\left|\vec{F}\right|$ (N/m^3) is the ultrasonic acoustic body force, l_{elev} the elevational resolution and l_{lat} the lateral resolution with these being in units of meters. Since the elastic modulus and the relaxed elastic modulus only differ by the axial resolution term, the elastic modulus may be calculated by dividing the relaxed elastic modulus by the axial resolution. In this case,

$$E = \frac{E_u}{l_{axial}}$$

where E(N/m^2) equals the elastic modulus, l_{axial} (m) the axial resolution, and E_u (N/m) the relaxed elastic modulus. To reiterate, the relaxed elastic modulus is equal to the spring constant calculated through the underdamped harmonic oscillator model divided by the axial resolution.

Calcium Digestion

In an attempt to correlate higher elastic modulus values with increased calcium concentration within the tissue constructs, a calcium digestion was performed on osteogenic tissue construct 2. The tissue construct was first removed from the culture plate and sealed in Tissue-Trek ® O.C.T. resin. Using a Cryo-Cut machine, the tissue constructs were cut into 400 micron slices and placed into separate test vials. Each of these pieces of tissue were dissolved in 0.5N HCl overnight in order to dissolve calcium out of the tissue constructs. These samples were allowed to sit overnight at 2ºC and approximately 24 hours later, were centrifuged at 500 rpm for 2 minutes. The supernatant was then extracted from each vial taking 30 micro liters of supernatant and placing it into a new vial with 570 micro liters of calcium reagent from the Calcium (CPC) LiquiColor® Test by Stanbio® (Boerne, Texas). Preparation of reagents was done following the directions that were included with the kit. Spectrophotometry was performed in triplicate of all tissue construct samples using 200 micro liters of supernatant/reagent mix per plate well. Known calcium concentrations were also included in the spectrophotometry in order to provide a standard to measure the unknown calcium samples against.

Results

Elastic Modulus Values

Elastic modulus values were reported for data in which curves were filtered using an R^2 value of 0.95 and filtered using an R^2 value of 0.8 (Figure 6). Values were not reported for the data set which was not filtered due to noisy data. This noisy data resulted in production of extremely high elastic modulus values. For the other two data sets, elastic modulus values were reported for each position imaged along all five constructs. Average elastic modulus values were calculated by averaging elastic modulus values for all points within each respective position. Elastic modulus values calculated by Pfeiler et. al. are located in Figure 7 for comparison.[4] All values in figure 6 have been log compressed due to the high order of magnitude differences in data. Actual elastic modulus values may be found in the appendix section.

4. Pfeiler, T. W., Sumanasinghe, R. D., Loboa, E. G., "Finite element modeling of 3D human mesenchymal stem cell-seeded collagen matrices exposed to tensile strain." *Journal of Biomechanics* Vol. 41, 2008, pp. 2289-22

Figure 6a. Elastic Modulus Values for Osteogenic Construct 1.

Calculated using R^2=0.95

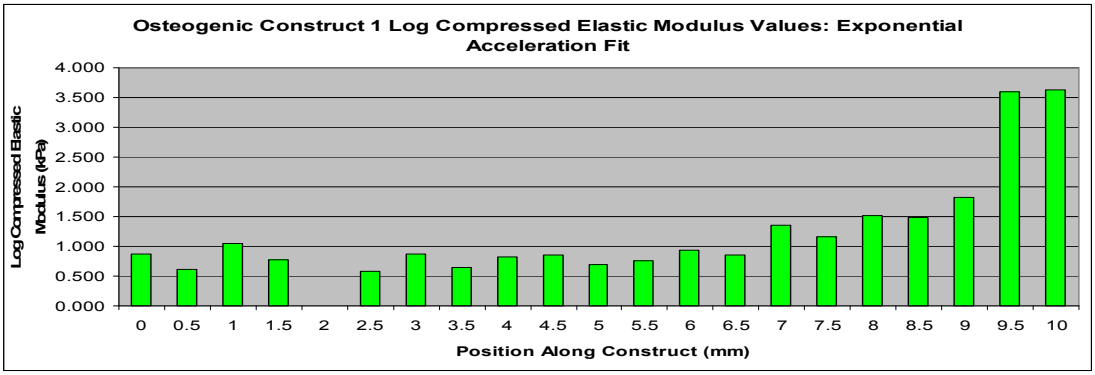

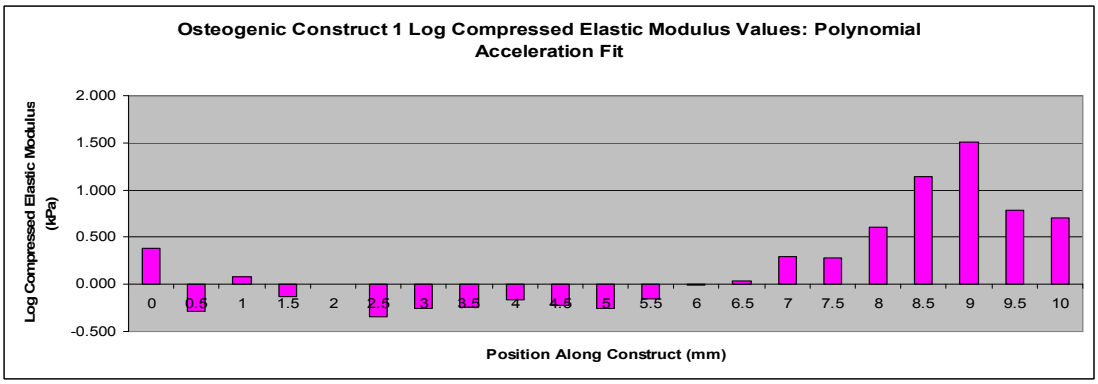

Calculated using R^2=0.8

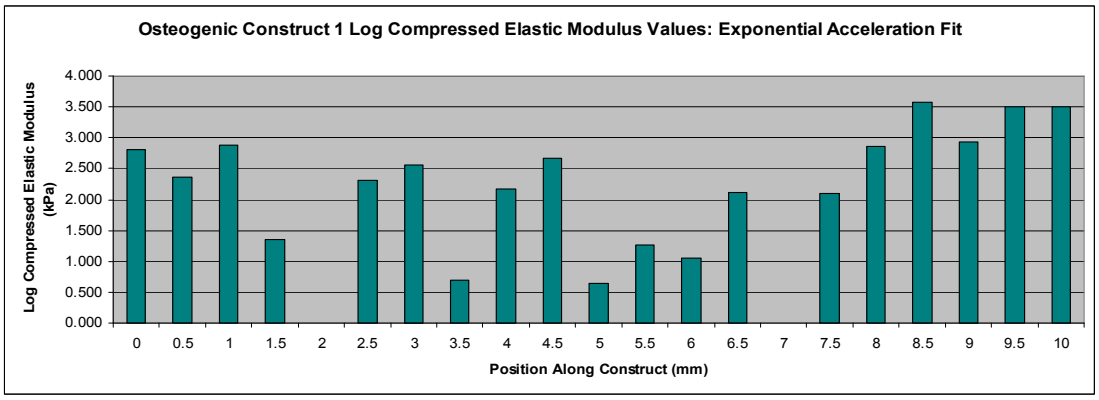

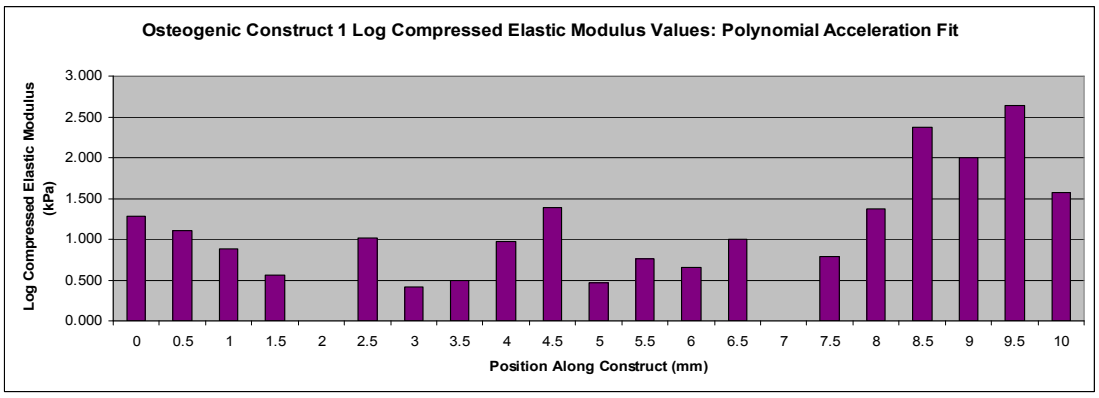

Figure 6b. Elastic Modulus Values for Osteogenic Construct 2.

Calculated using R^2=0.95

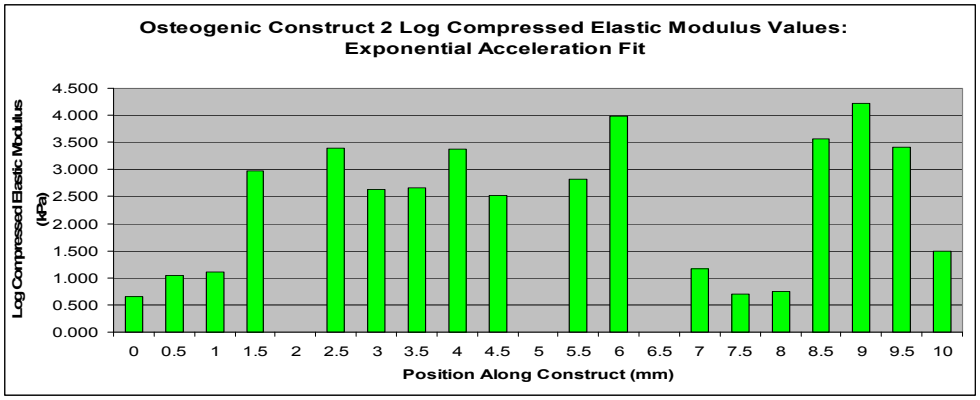

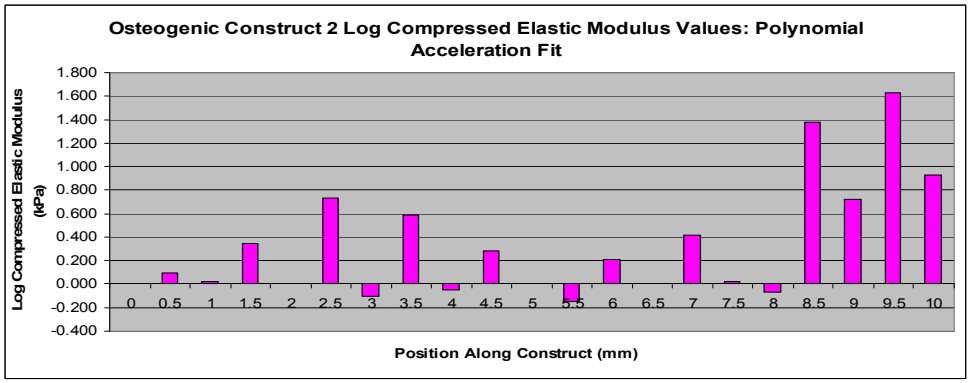

Calculated using R^2=0.8

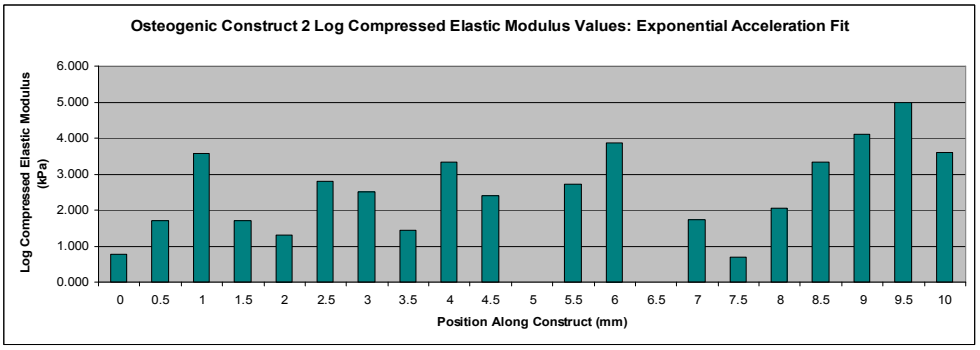

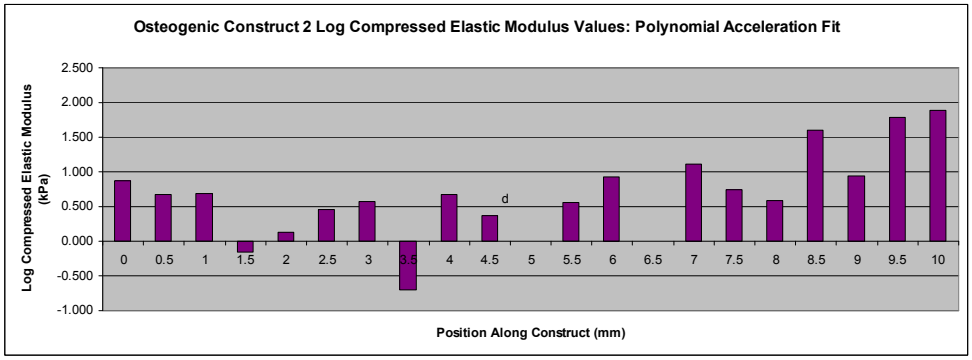

Figure 6c. Elastic Modulus Values for Osteogenic Construct 3.

Calculated using R^2=0.95

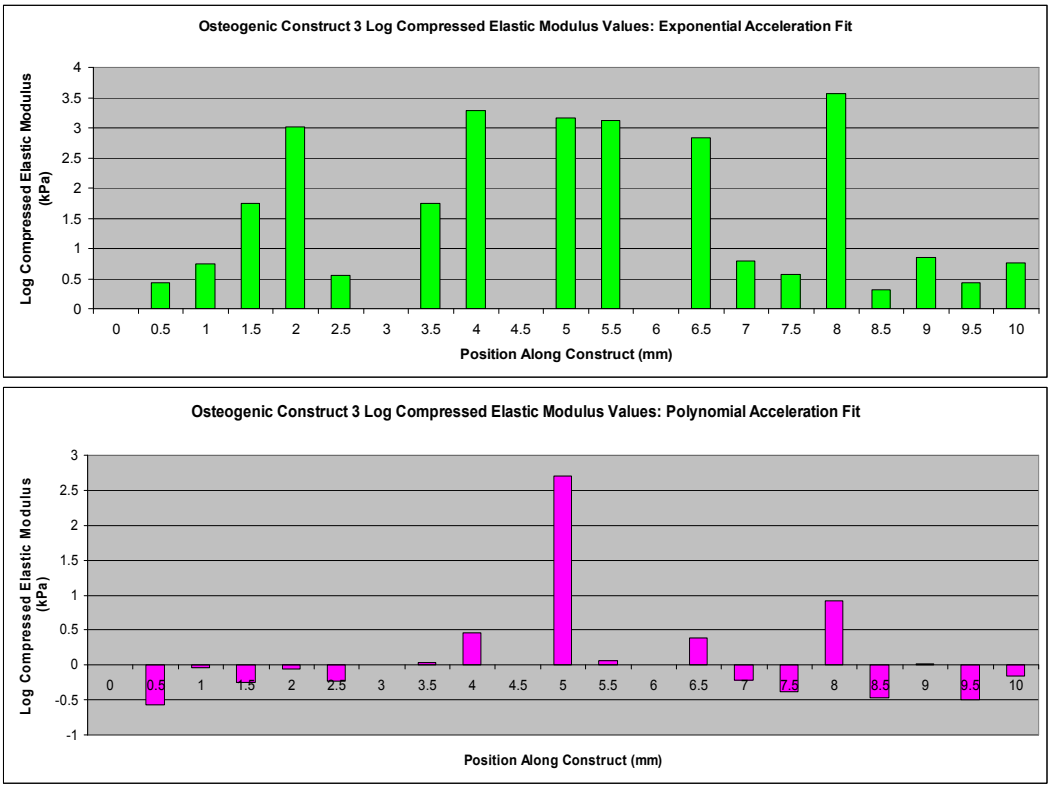

Calculated using R^2=0.8

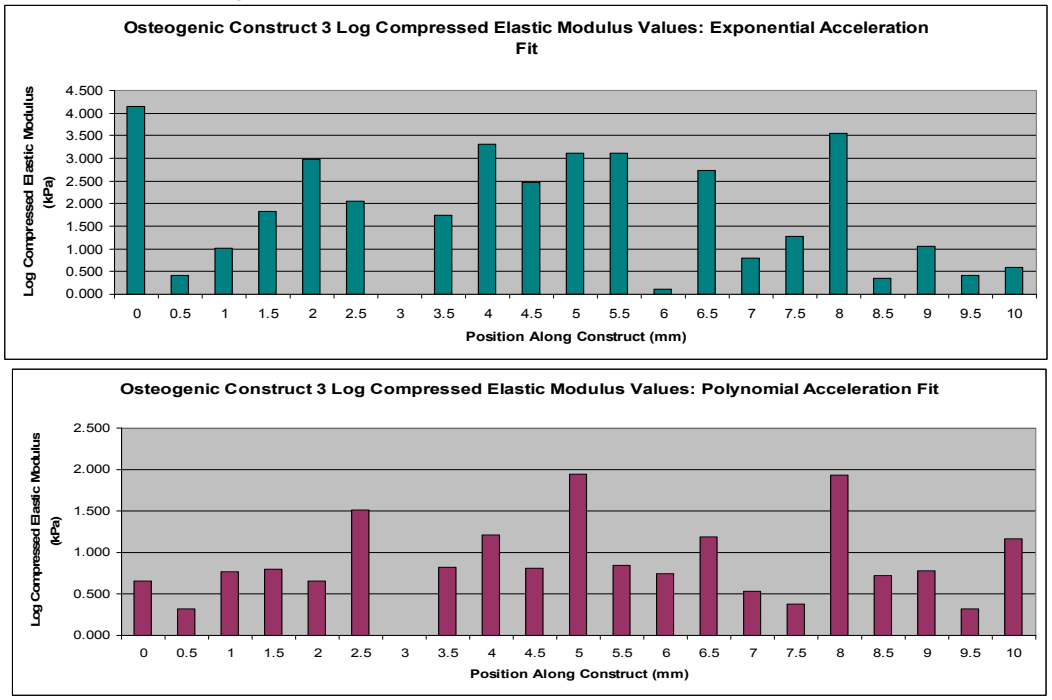

Figure 6d. Elastic Modulus Values for Complete Growth Media Construct 1.

Calculated using R^2=0.95

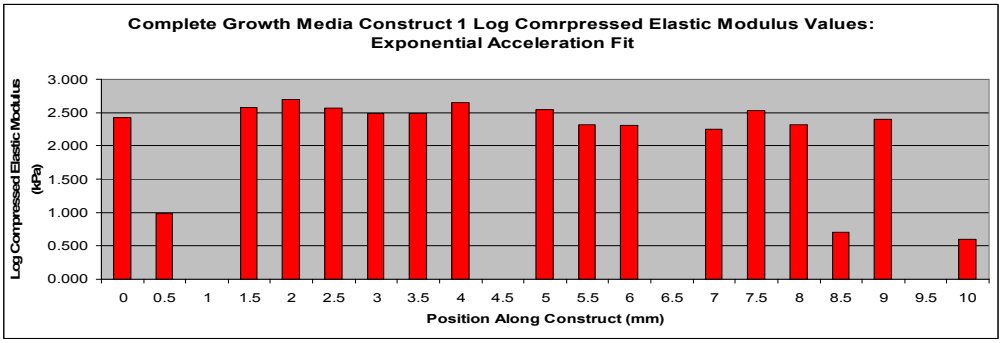

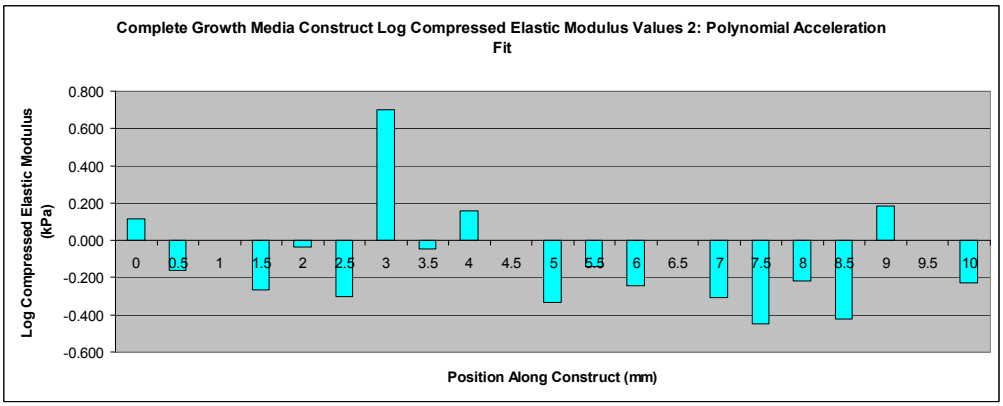

Calculated using R^2=0.8

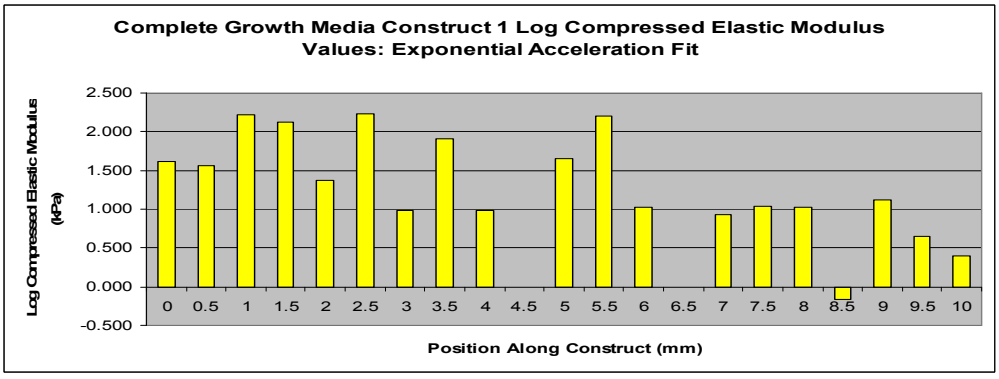

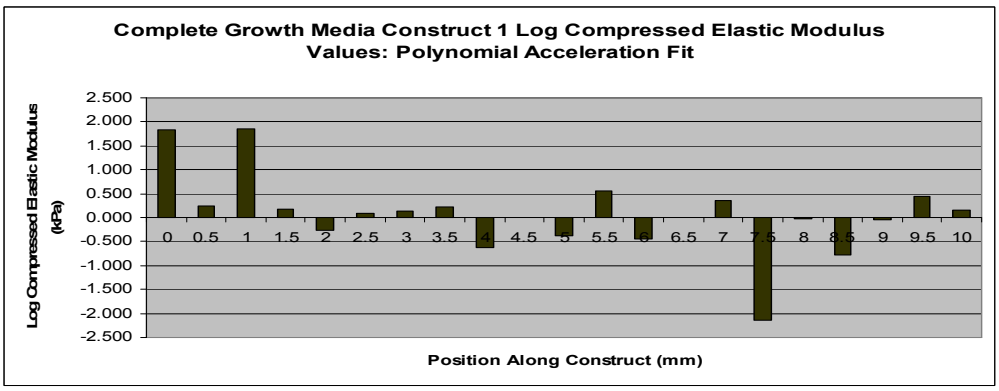

Figure 6e. Elastic Modulus Values for Complete Growth Media Construct 2.

Calculated using R^2=0.95

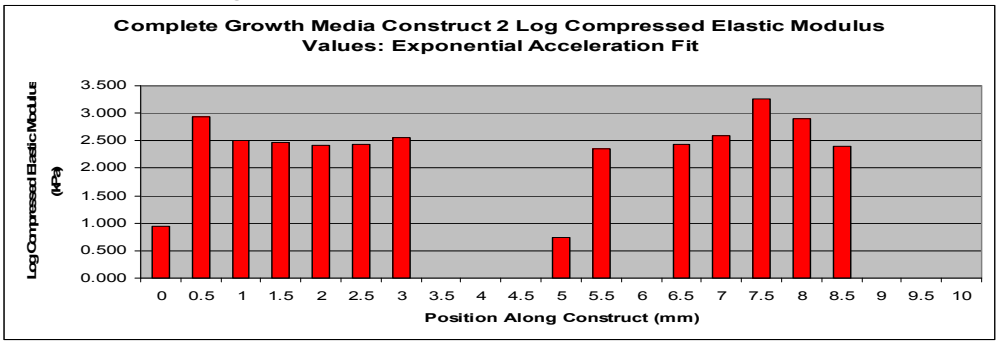

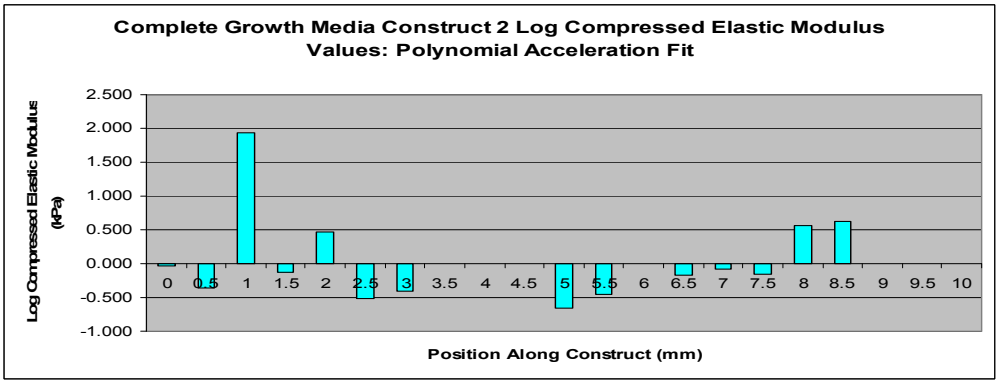

Calculated using R^2=0.8

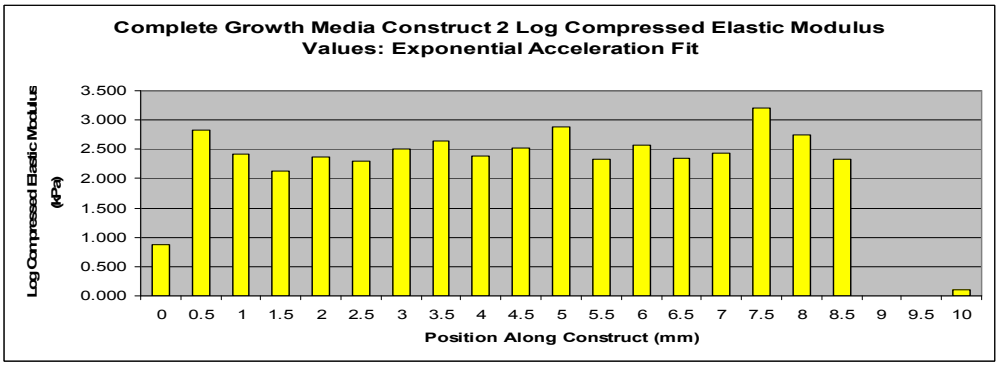

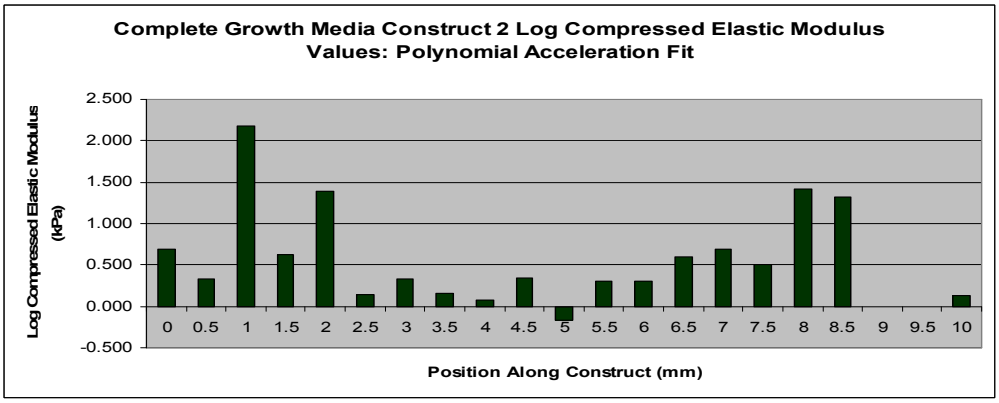

Figure 7. Elastic Modulus Values Calculated by Pfeiler et. al.

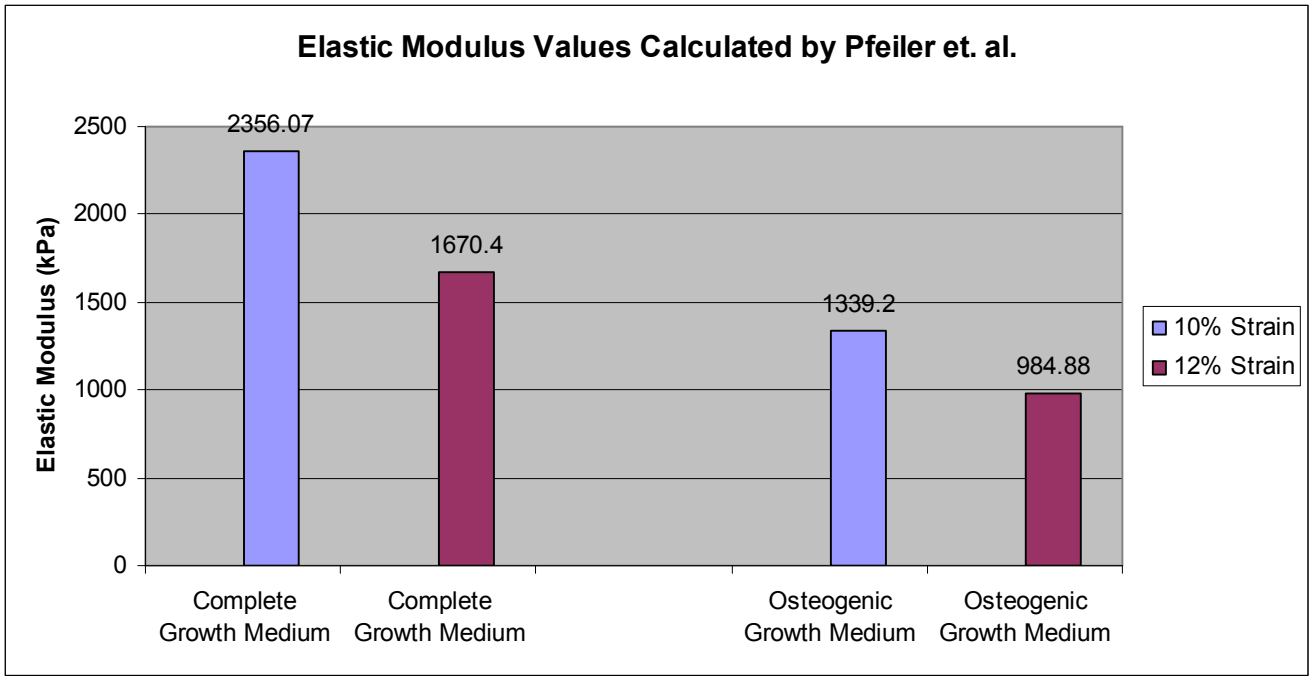

Image rendering

Elastic modulus images were produced from processed data. These images show areas or points within the tissue constructs which have higher and lower areas of the elastic modulus. For establishment of a reference point, elastic modulus images were superimposed into B-mode images. Images were produced for all five tissue constructs. Images were created from filtered data produced earlier during data processing. These data sets include those in which data curves were filtered using an R^2 value of 0.8 and those selected for using an R^2 value of 0.95. Curves without filtering were not imaged. Within data sets for each tissue construct, acceleration of the tissue constructs during force excitation was calculated 2 separate ways; fitting an increasing exponential curve and fitting a polynomial curve. This analysis resulted in four different stiffness images produced for each of the five constructs. These images are beneficial in providing a quick, visual way of determining the areas of higher Elastic modulus within the tissue constructs. Color bars on stiffness images represent Elastic modulus values in units of Pascals. Due to the high order magnitude differences in this data, a log compression was performed. These elastic modulus images are found in Figure 8.

Figure 8a.

Osteogenic Tissue Construct 1

Stiffness Images Filtering Curves Using $R^2 = 0.95$

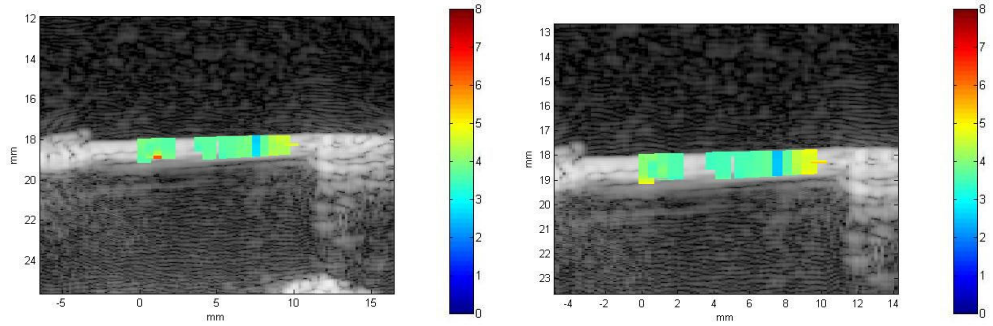

Increasing Exponential Fit

Polynomial Fit

Stiffness Images Filtering Curves Using $R^2 = 0.8$

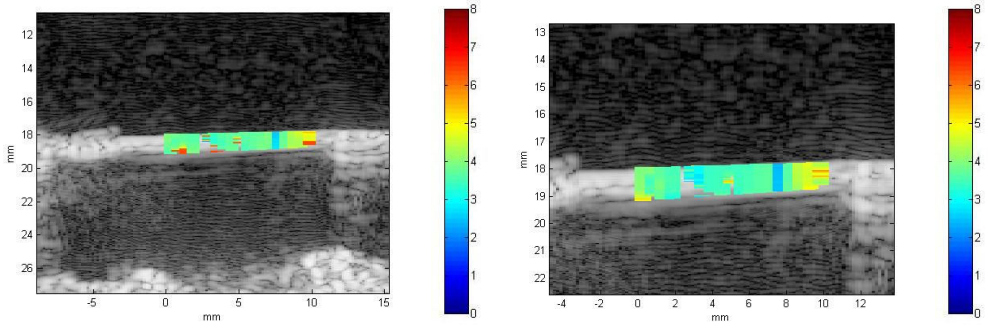

Increasing Exponential Fit

Polynomial Fit

Colorbars indicate log compressed elastic modulus values in units of Pascals.

Figure 8b.

Osteogenic Tissue Construct 2

Stiffness Images Filtering Curves Using $R^2 = 0.95$

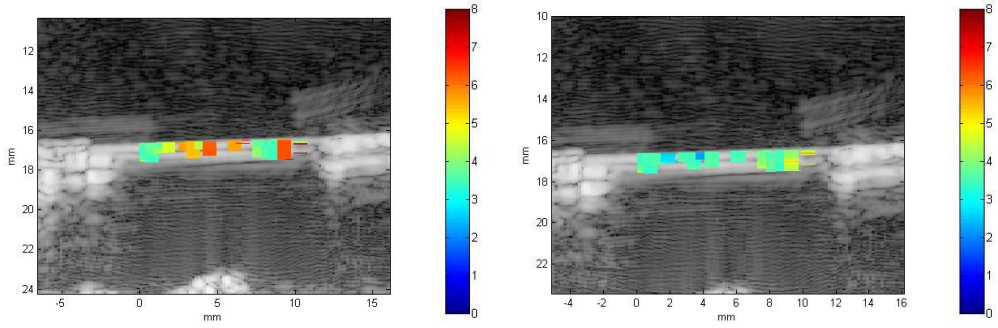

Increasing Exponential Fit

Polynomial Fit

Stiffness Images Filtering Curves Using $R^2 = 0.8$

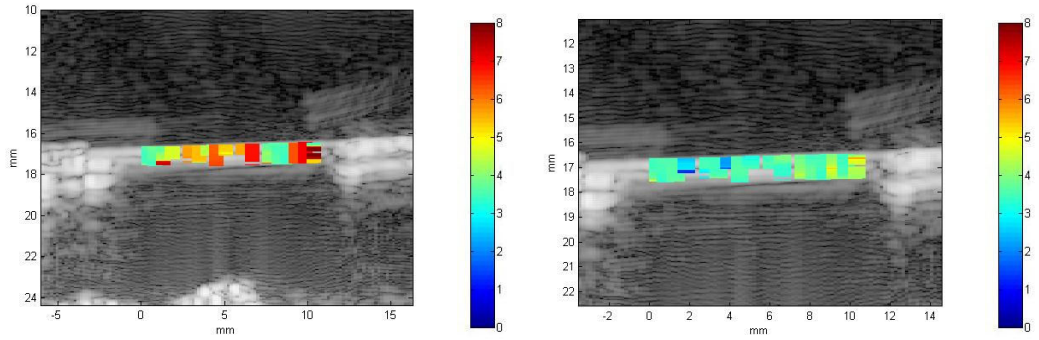

Increasing Exponential Fit

Polynomial Fit

Colorbars indicate log compressed elastic modulus values in units of Pascals.

Figure 8c.

Osteogenic Tissue Construct 3

Stiffness Images Filtering Curves Using $R^2 = 0.95$

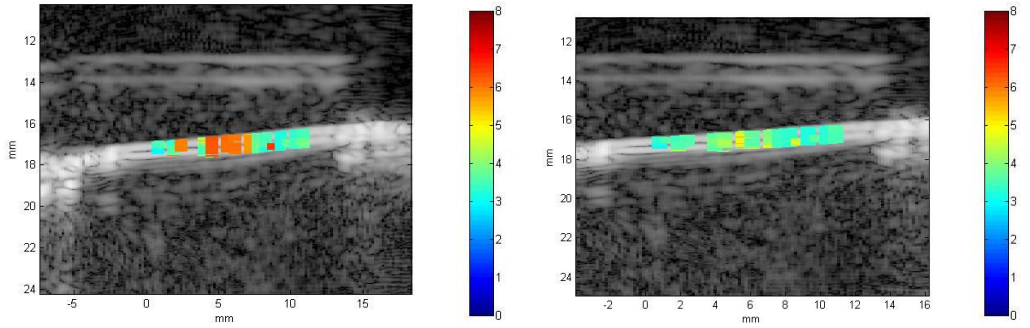

Increasing Exponential Fit Polynomial Fit

Stiffness Images Filtering Curves Using $R^2 = 0.8$

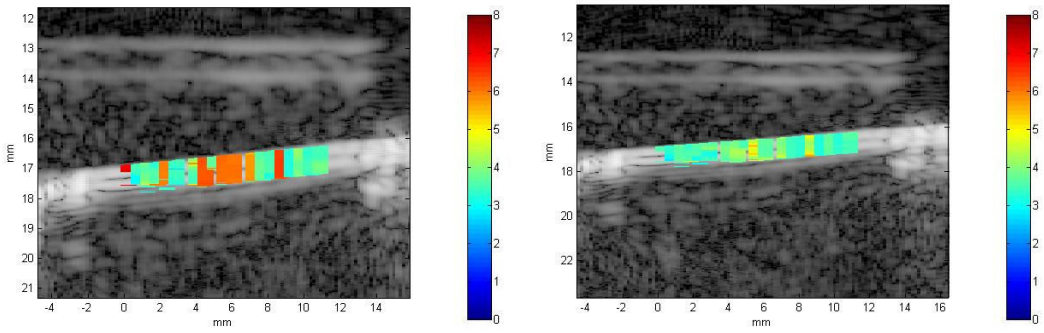

Increasing Exponential Fit Polynomial Fit

Colorbars indicate log compressed elastic modulus values in units of Pascals.

Figure 8d.

Complete Growth Media Tissue Construct 1

Stiffness Images Filtering Curves Using $R^2 = 0.95$

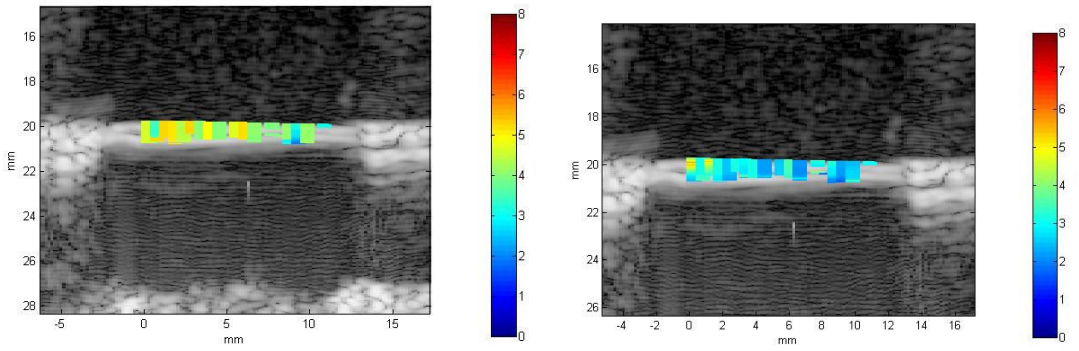

Increasing Exponential Fit Polynomial Fit

Stiffness Images Filtering Curves Using $R^2 = 0.8$

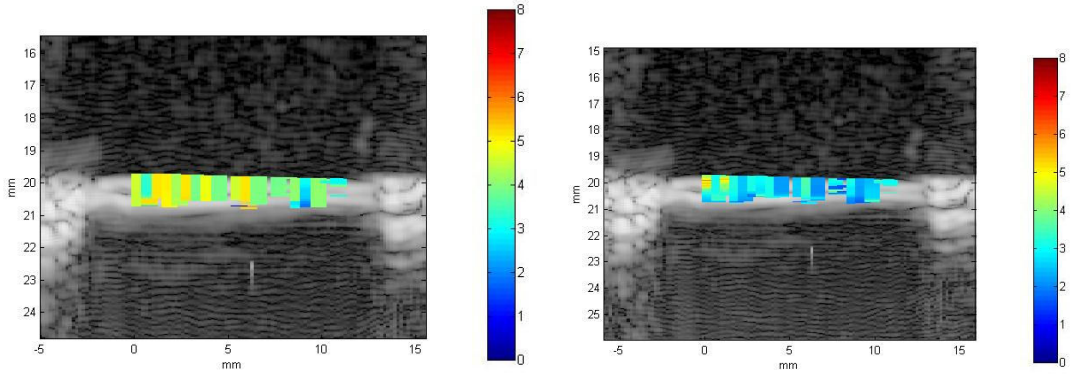

Increasing Exponential Fit Polynomial Fit

Colorbars indicate log compressed elastic modulus values in units of Pascals.

Figure 8e.

Complete Growth Media Tissue Construct 2

Stiffness Images Filtering Curves Using $R^2 = 0.95$

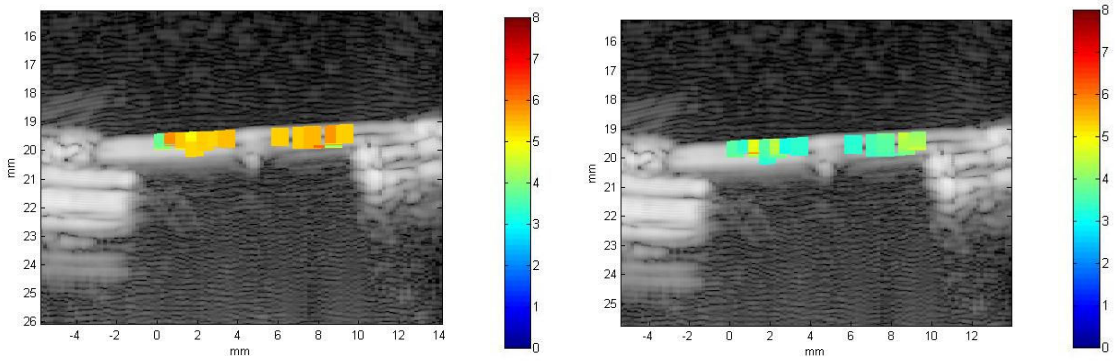

Increasing Exponential Fit Polynomial Fit

Stiffness Images Filtering Curves Using $R^2 = 0.8$

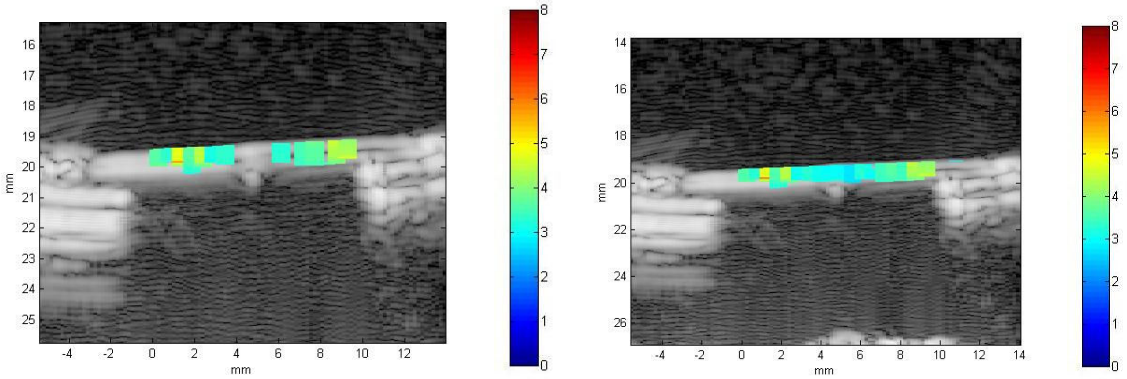

Increasing Exponential Fit Polynomial Fit

Colorbars indicate log compressed elastic modulus values in units of Pascals.

Calcium Digestion

Calcium digestion performed on osteogenic tissue construct 2 was successful in showing areas in the tissue construct in which there was higher and lower areas of calcium. Higher calcium concentration was linked to higher elastic modulus values along the tissue construct. When plotting elastic modulus values against calcium concentration for each lateral position, there were some similarities between higher elastic modulus values and higher calcium concentrations, although there were some extreme outlying points. Elastic modulus data created using increasing exponential fit and polynomial fit for acceleration along with filtering data using an R^2 value of 0.95 and R^2 value of 0.8 was plotted against calcium concentrations. The relation between higher elastic modulus and higher calcium concentration was seen in both acceleration calculation methods and R^2 filtering methods. Figure 9 shows calcium concentrations along the length of osteogenic construct 2 and actual values of calcium concentration reported. In figure 10, calcium concentration was plotted against elastic modulus values.

Many difficulties still remain in being able to correctly correlate elastic modulus calculations to calcium concentrations and their correct position along the tissue construct. These issues can be attributed to the degradation of these samples over time along with contraction of these samples as they dry out. Several months had passed from the time these constructs had been imaged to the time the calcium digestion was performed. In future analysis, it would be better to perform the calcium digestion much sooner after imaging of these tissue constructs.

Figure 9. Calcium Digestion Results Osteogenic Construct 2

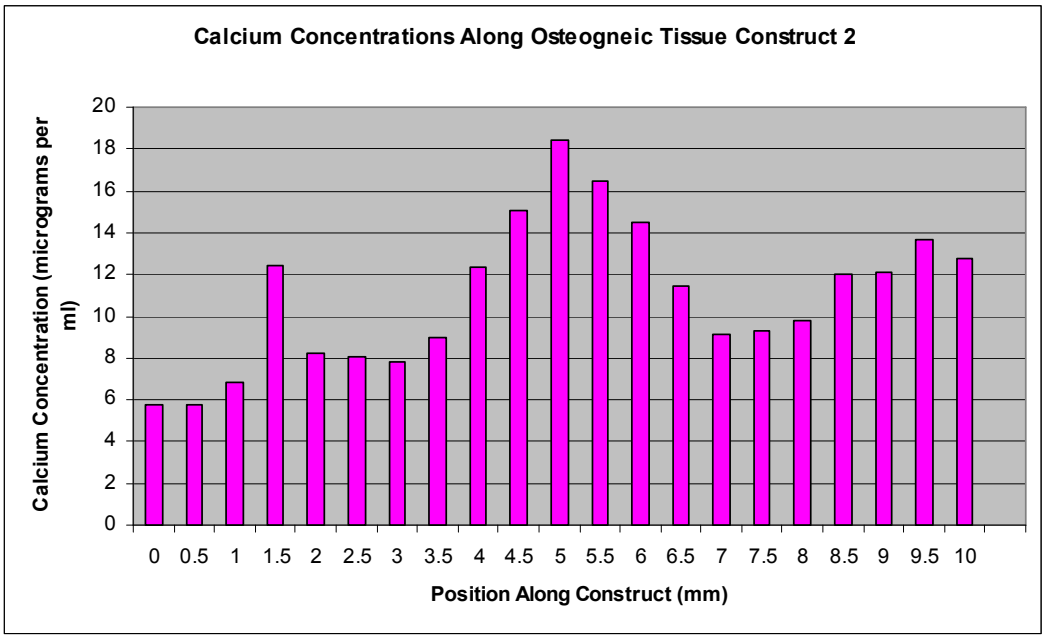

Position Along Construct (mm)	Calcium Concentration (µg/ml)
0	5.775
0.5	5.775
1	6.811
1.5	12.423
2	8.225
2.5	8.081
3	7.847
3.5	9.000
4	12.306
4.5	15.027
5	18.396
5.5	16.477
6	14.477
6.5	11.441
7	9.117
7.5	9.297
8	9.811
8.5	11.982
9	12.099
9.5	13.631
10	12.793

Figure 10 Elastic Modulus vs. Calcium Concentration

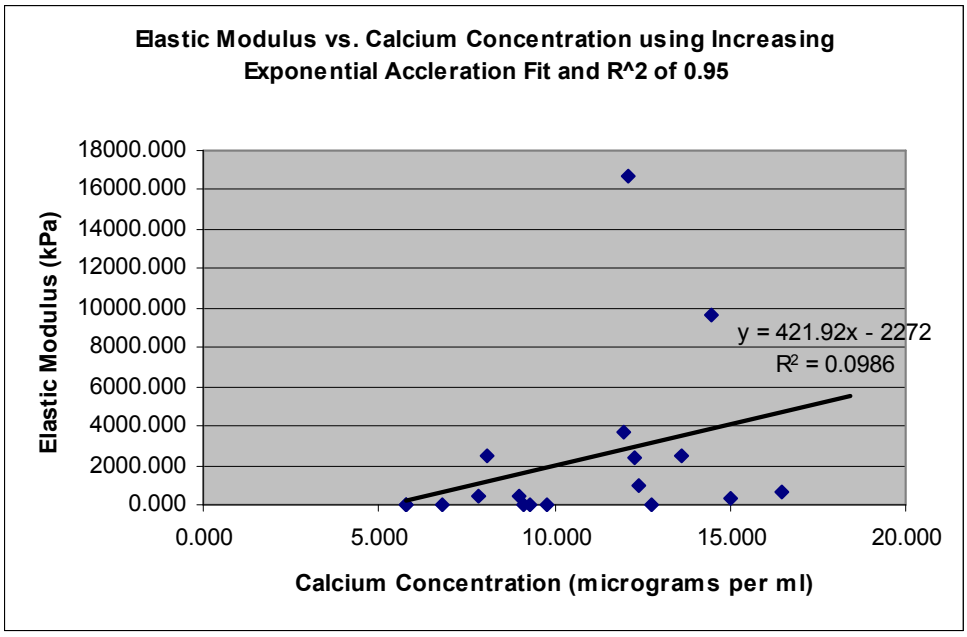

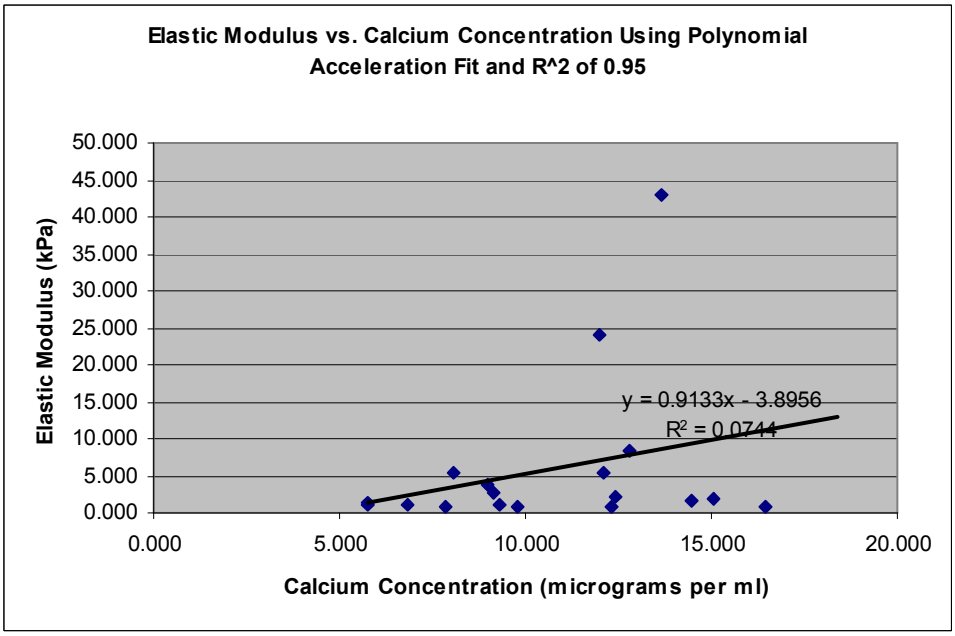

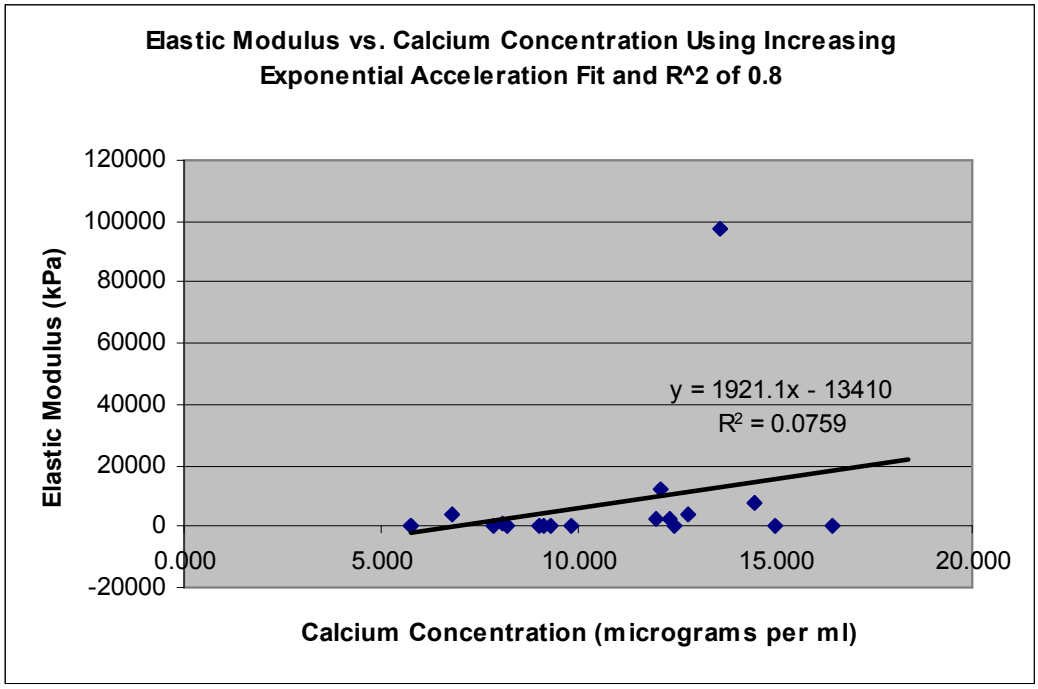
Elastic Modulus vs. Calcium Concentration Using Increasing Exponential Acceleration Fit and R^2 of 0.8
Elastic Modulus (kPa)
120000
100000
80000
60000
40000
20000
0
-20000
0.000
5.000
10.000
15.000
20.000
y = 1921.1x - 13410
R2 = 0.0759
Calcium Concentration (micrograms per ml)

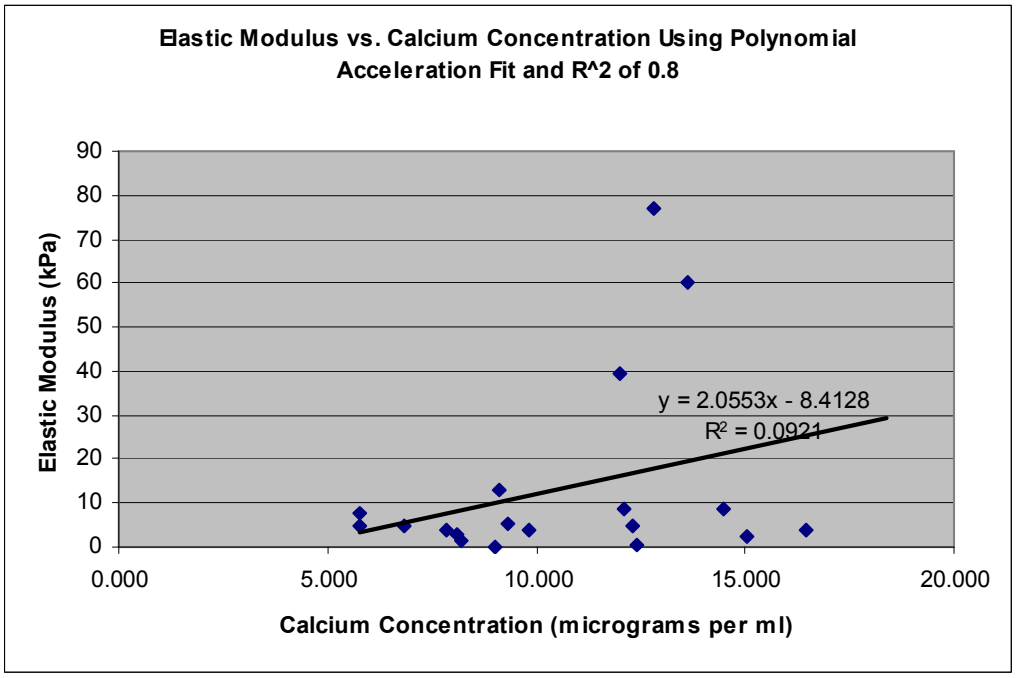
Elastic Modulus vs. Calcium Concentration Using Polynomial Acceleration Fit and R^2 of 0.8
Elastic Modulus (kPa)
90
80
70
60
50
40
30
20
10
0
0.000
5.000
10.000
15.000
20.000
y = 2.0553x - 8.4128
R2 = 0.0921
Calcium Concentration (micrograms per ml)

Mean Elastic Modulus Values:

After filtering of curves, elastic modulus values were first calculated for constructs grown in osteogenic media using an increasing exponential fit to calculate acceleration data. A wide range of elastic modulus values were found. These values ranged from on the low end of being in the order of 1-10 kilopascals to even as high as several thousand kilopascals on the upper end. Such a wide variation in the magnitude of elastic modulus values could be attributed to areas of calcification within the constructs that would result in higher elastic modulus values. Comparing elastic modulus values calculated from filtered data using a high R^2 value equal to 0.95 and then a lower R^2 value equal to 0.8, it was found in general a lower R^2 value resulted in a higher calculation of elastic modulus. This can be attributed to an increase of noisy points used in elastic modulus calculation. When using a polynomial fit for acceleration values, a much lower elastic modulus value was calculated. With only a few exceptions, most of these values were calculated to be on the order of hundreds or thousands of Pascals. Values, with the exception of a few outlier points, were fairly consistent. These consistent elastic modulus values calculated were attributed to much more consistent acceleration values that were calculated when using a polynomial fit. Increasing exponential fit acceleration values showed much more variation between points. Elastic modulus values which used an increasing exponential fit were close to ones reported in previous work while values calculated using a polynomial fit being much lower.

Elastic modulus values were also calculated for constructs grown in complete growth media using an increasing exponential fit to calculate acceleration. Using this method, with

only a few exceptions, values were calculated to be on the order of several hundred kilopascals. More consistent elastic modulus values were calculated in these tissue constructs than those grown in osteogenic media. Variations along the tissue constructs were not as extreme as with tissue constructs grown for osteogenic differentiation. These constructs would be expected to be more homogeneous than those grown in osteogenic media due to a lack of osteogenic differentiation and calcium deposition in the complete growth media constructs. It is these calcium deposits that result in higher elastic modulus values in osteogenic tissue constructs. A polynomial fit was next used to calculate acceleration values. Using this method, calculated elastic modulus values were on the order of several hundred Pascals. Elastic modulus values, due to more uniform acceleration values calculated using this method, were consistent overall except for outlying points. In fact, very little differences were found between elastic modulus values in tissue constructs grown in osteogenic media and complete growth media using the polynomial fit for acceleration. As with the tissue constructs grown in osteogenic media, the elastic modulus values calculated using the increasing exponential fit gave values very close to those reported in earlier work, where values using the polynomial fit were much lower than those reported in earlier work.

Elastic Modulus Images:

Elastic modulus images were successful in highlighting specific lateral and axial areas within tissue constructs which had higher or lower areas of Elastic modulus values. These images will be useful in indicating areas within the tissue constructs where calcium deposits, which indicate osteogenic differentiation, are located since calcium has a higher elastic modulus value than the other materials in the construct. It was also noted that although the increasing exponential acceleration fit and polynomial acceleration fit gave very different

elastic modulus values, both acceleration methods generally predicted the same differences of elastic modulus within the tissue constructs. This was quite visible when comparing images of elastic modulus.

Elastic modulus images produced in which filtering was used resulted in a large number of data curves removed. Removed curves do not appear on the Elastic modulus images. In the data set in which all curves were included, there was concern in the accuracy of the values which were allowed in these. Due to extremely high elastic modulus values calculated in the data set with no filtering, these images and elastic modulus values were not included. These removed curves still remain an issue in this imaging modality for production of images. These curves, which are removed during filtering, are removed since they do not follow an increasing exponential while constant strain is applied. This model was selected for its description of viscoelastic behavior. These excitation curves are used to calculate the tissue acceleration values. Therefore in curves which do not fit the exponential model, the calculation of acceleration may be inaccurate since an increasing exponential curve is forced on data which does not exhibit such a response. This leads to a concern regarding the accuracy of elastic modulus in some values in images including all curves. Although acceleration values were also calculated for curves using a polynomial curve to obtain a constant acceleration value, there was still concern for accuracy since a polynomial equation does not model the response of viscoelatic materials under constant stress. Even in cases where the polynomial fit was used for acceleration data, filtering was still done using an increasing exponential.

Even though acceleration data of the tissue is a locally determined parameter, the oscillation frequency used is a parameter that is global to each construct. This is attributed to

the fact that the oscillation frequency is dependent upon the properties of the entire construct. Thus calculation of elastic modulus values via the underdamped harmonic oscillation model requires the input of both global and local parameters. It can not therefore be said the underdamped harmonic oscillation model completely uses only local parameters in calculation of local elastic modulus values.

The differential equation describing the underdamped harmonic oscillation model has three coefficients within the differential equation to describe the behavior of the oscillating system. These include the mass, damping, and spring constant coefficients. Calculation of this elastic modulus value in this study only required use of the mass and spring constants and did not use the damping coefficient in the calculation for elastic modulus. This coefficient which was neglected in these calculations does provide additional information about the properties of the tissue. Use of this damping coefficient in calculation for elastic modulus may offer additional information about the mechanical properties of the constructs.

F. Conclusions

When comparing values from this study to previous work performed by Pfeiler et. al., similarities in elastic modulus values were found in calculations which used an increasing exponential fit. Elastic modulus values calculated using the polynomial curve fit for acceleration gave much lower values than those calculated in earlier work. However, it must be pointed out that the tensile test performed in earlier work was completely different from the test performed in this experiment. Pfeiler et. al. utilized a tensile test, measuring the tensile strength of the tissue constructs. In the tensile test the construct was stretched on both ends and the accompanying stress and strain were measured. In the MSSER experiments, an

acoustic compression force was applied axially to the construct with deformation and oscillation frequency of the tissue constructs used for elastic modulus calculation. This compression force may also be linked to a tension force experienced on the ends of the tissue construct when compression is occurring along the length of the tissue constructs. These two methods are testing two completely different mechanical responses of the tissue constructs. Another difference that existed between constructs used by Pfeiler et. al. and those used in this study was there was a 10% and 12% strain applied to those used by Pfeiler et. al. However, no strain was applied to the constructs used in this study. These differences in strain can also result in differences in elastic modulus calculations. Therefore, it can not be concluded which method for acceleration value is best by just comparing data from Pfeiler et. al. to data from this study due to the many differences in experimental setup between the two studies..

Although MSSER shows potential for being useful in determining the mechanical properties of tissue constructs, much work is still needed to perfect the methods. One issue that remains is noise within the system, specifically during tissue construct excitation. Noise can be attributed to motion within the construct and even noise generated within the fluid which the cells are contained including reverberations from within the container. This presents a problem when trying to calculate the acceleration value of the tissue during excitation. This acceleration value is an important parameter in calculating the mass constant. The problem associated with noisy data is difficulty in calculating a correct acceleration value. Noisy data can result in an incorrect acceleration calculation.

Another issue at the forefront is developing a better method for calculation of the acceleration of the tissue. For purpose of comparing, two different methods were used for

the acceleration calculation. Two different arguments regarding which is best to use may be made; although the polynomial curve fits the excitation data better, an increasing exponential is a better mathematical model of how viscoelastic materials are to respond under a constant force. The first method, fitting an increasing exponential curve to excitation data, was selected since this equation is used to describe the change in strain of a viscoelastic material while under constant stress. Upon taking the second derivative, an equation for acceleration is produced. Plugging time positions into the equation gives the acceleration for each point throughout the excitation period. These values, although mostly on the same order of magnitude, must be averaged together to give an acceleration to use in calculations. In an effort to calculate a constant acceleration value, a polynomial fit was used on excitation data. Taking the second derivative of this fitted polynomial curve gave a constant acceleration value. The polynomial curve incidentally fit the excitation data better, but produced much lower values of elastic modulus when compared with those produced by the increasing exponential fit. These elastic modulus values were also less consistent with those that were reported by Pfeiler et. al. However, the tests performed in earlier work were completely different from the MSSER experiments; therefore, it is possible for much different elastic modulus values to be found between earlier methods and those investigated in this study.

Elastic modulus values were very sensitive to the acceleration calculation values using an increasing exponential fit for acceleration of the tissue. This did raise some concern in accuracy of this model since an average acceleration was used in the elastic modulus calculation due to this model yielding multiple acceleration values throughout the tissue excitation period. However, these elastic modulus values averaged to yield a mean acceleration value to use in the calculation for mass were all on the same order of magnitude

having little effect on the elastic modulus calculation. In Figure 11, the elastic modulus value was calculated in osteogenic construct 1 using an increasing exponential fit for acceleration calculation for the lateral position at 4 mm and axial depth of 19.1 mm. The elastic modulus value at this point was calculated using the mean acceleration, mean acceleration plus one standard deviation and acceleration minus one standard deviation. This standard deviation was derived from all tissue acceleration values throughout the excitation period of the tissue. Differences in elastic modulus values varied by 2 kilopascals.

Figure 11 elastic modulus values and acceleration

	Acceleration m/s^2	Elastic Modulus kPa
Mean Accel. + 1 Std. Dev.	7.8674347x10^-4	2197
Mean Acceleration	7.8632x10^-4	2198
Mean Accel - 1 Std. Dev.	7.8589653x10^-4	2199
Standard Deviation	4.2347x10^-7	

1. Bernacki SH, Wall ME, and Loboa EG. 2008. Isolation of human mesenchymal stem cells from bone and adipose tissue. Methods Cell Biol.;86:257-78.

2. Sumanasinghe RD, Bernacki SH, and Loboa EG. 2006. Osteogenic differentiation of human mesenchymal stem cells in collagen matrices: effect of uniaxial cyclic tensile strain on bone morphogenetic protein (BMP-2) mRNA expression. Tissue Eng. Dec;12(12):3459-65.

3. Mauldin, F. W. Jr., Haider, M. A., Loboa, E. G., Behler, R. H., Euliss, L. E., Pfeiler, T. W., Gallippi, C. M., "Monitored Steady-State Excitation and Recovery (MSSER) Radiation Force Imaging Using Viscoelastic Models" *IEEE Transaction on Ultrasonics, Ferroelectrics, and Frequency Control*,Vol. 55, No. 7, 2008, pp. 1597-1610.

4. Pfeiler, T. W., Sumanasinghe, R. D., Loboa, E. G., "Finite element modeling of 3D human mesenchymal stem cell-seeded collagen matrices exposed to tensile strain." *Journal of Biomechanics* Vol. 41, 2008, pp. 2289-22

Chapter 5: Summary and Future Work

In the future, more study of the damping coefficient in the damped harmonic oscillation model needs to be done. This parameter, excluded from calculations in this study could provide more information about the mechanical properties of these tissue constructs. This additional information may lead to a better calculation of the elastic modulus. Another important addition to this study would be confirming the mass approximations calculated using both the increasing exponential and polynomial acceleration models. This would be completed by slicing the tissue constructs into approximately 500 micron slices, the later resolution size of the imaging system, allowing the slices to dry, and finally measuring the mass. The mass of the tissue would be compared to estimated masses in order to determine which acceleration model calculation best predicts the mass of these tissue construct slices. Performing calcium digestion on all tissue constructs would also need to be performed in the future. In addition, performing micro CT on all samples will also be useful in validating the methods in this study. Micro CT is capable of detecting calcium deposits along the length of the tissue construct.

Continuing work with this study will also need to address the problem with using the oscillation frequency in elastic modulus calculations. The underdamped harmonic oscillation model investigated in this study relies on, for elastic modulus calculation, locally derived focal displacements and the oscillation frequency of the tissue construct. Oscillation frequency depends on the mechanical properties over a range of the construct. Therefore, it cannot be said that elastic modulus values calculated in this study are completely local

measurements. One idea for eliminating this dependence on adjacent tissue properties would be to remove the oscillation from the tissue construct. This could be accomplished by placing a substrate below this tissue construct. Leaving the plastic membranes in tact below the tissue construct may, in fact, be enough to eliminate the oscillation which currently occurs at force cessation. Tissue constructs could first be imaged with membranes still in tact and them imaged with a substrate placed below the membrane to compare how well oscillation is removed. Elimination of the damped harmonic oscillation occurring after force cessation will require modification of the current model. It is possible the overdamped harmonic oscillation models may be more of an appropriate model to use once oscillation is removed. Removal of the damped harmonic oscillation occurring after force cessation may allow for the use of the Voigt model of viscoelasticity.

Future work will also require better calculation of tissue acceleration data. Currently, a large number of data points are removed leaving holes in the data. These data points are removed due to the noisiness of these points. Production of a noise filter and better fitting of excitation data will help in increasing the number of curves which are not filtered. A filter capable of not only removing noise but making an estimation of what the correct excitation curve should look like may also be necessary. Other methods may also need to be developed to calculate the acceleration data.

Appendix

Average Elastic Modulus Values Created Filtering Data with an R^2 value of 0.95.

Osteogenic Construct 1 Elastic Modulus Values

Position mm	Exponential Fit kPa	Polynomial Fit kPa
0	7.386	2.409
0.5	4.052	0.518
1	11.353	1.209
1.5	5.926	0.744
2		
2.5	3.851	0.451
3	7.328	0.560
3.5	4.478	0.570
4	6.598	0.685
4.5	7.232	0.606
5	4.870	0.562
5.5	5.666	0.708
6	8.579	0.986
6.5	7.233	1.085
7	22.315	1.972
7.5	14.234	1.926
8	32.310	4.000
8.5	30.811	13.848
9	65.763	32.532
9.5	3888.000	6.037
10	4180.000	5.030

Osteogenic Construct 2 Elastic Modulus Values

Position mm	Exponential Fit kPa	Polynomial Fit kPa
0	4.564	1.007
0.5	11.056	1.248
1	12.902	1.063
1.5	958.980	2.213
2		
2.5	2476.500	5.412
3	431.120	0.784
3.5	462.630	3.866
4	2428.600	0.889
4.5	337.500	1.915
5		
5.5	649.350	0.711
6	9677.800	1.610
6.5		
7	14.941	2.617
7.5	5.075	1.042
8	5.584	0.852
8.5	3637.100	23.950
9	16735.000	5.275
9.5	2541.500	42.947
10	31.045	8.492

Osteogenic Construct 3 Elastic Modulus Values

Position mm	Exponential Fit kPa	Polynomial Fit kPa
0	2.749	0.268
0.5	5.624	0.923
1	55.093	0.571
1.5	1039.000	0.869
2	3.525	0.592
2.5		
3	56.146	1.091
3.5	1925.400	2.933
4		
4.5	1456.000	513.932
5	1311.200	1.166
5.5		
6	686.610	2.459
6.5	6.145	0.606
7	3.630	0.423
7.5	3713.100	8.418
8	2.060	0.345
8.5	7.145	1.040
9	2.749	0.318
9.5	5.714	0.686
10		

Complete Growth Media Construct 1
Elastic Modulus Values

Position	Exponential Fit	Polynomial Fit
mm	kPa	kPa
0	267.3	1.304
0.5	9.678	0.690
1		
1.5	378	0.545
2	493.85	0.921
2.5	370.8	0.498
3	305.26	5.012
3.5	307.42	0.897
4	440.69	1.443
4.5		
5	352.5	0.467
5.5	209.9	0.721
6	204.2	0.567
6.5		
7	179.9	0.492
7.5	340.6	0.355
8	210.9	0.603
8.5	5.03	0.380
9	255	1.522
9.5		
10	3.9454	0.590

Complete Growth Media Construct 2
Elastic Modulus Values

Position	Exponential Fit	Polynomial Fit
mm	kPa	kPa
0	8.890	0.945
0.5	865.940	0.445
1	321.050	86.054
1.5	298.760	0.759
2	265.300	2.951
2.5	272.360	0.300
3	361.110	0.392
3.5		
4		
4.5		
5	5.387	0.220
5.5	226.920	0.350
6		
6.5	267.740	0.677
7	395.710	0.836
7.5	1806.400	0.688
8	787.560	3.669
8.5	250.430	4.226
9		
9.5		
10		

Mean Elastic Modulus Values Created Filtering Data with an R^2 value of 0.8.

Osteogenic Construct 1 Elastic Modulus Values		
Position	Exponential Fit	Polynomial Fit
mm	kPa	kPa
0	638.760	19.278
0.5	229.950	12.916
1	745.790	7.585
1.5	22.126	3.681
2		
2.5	206.260	10.182
3	361.370	2.560
3.5	4.910	3.151
4	146.000	9.279
4.5	466.940	24.171
5	4.401	2.897
5.5	18.116	5.674
6	11.174	4.467
6.5	130.770	10.145
7		
7.5	123.370	6.187
8	718.900	23.314
8.5	3700.200	233.200
9	858.190	100.740
9.5	3145.200	431.980
10	3194.600	37.898

Osteogenic Construct 2 Elastic Modulus Values

Position	Exponential Fit	Polynomial Fit
mm	kPa	kPa
0	5.759	7.468
0.5	51.658	4.646
1	3741	4.794
1.5	50.245	0.70038
2	20.039	1.354
2.5	616.5	2.908
3	327.96	3.6814
3.5	28.005	0.1987
4	2198.2	4.709
4.5	245.35	2.3467
5		
5.5	540.95	3.613
6	7441.3	8.485
6.5		
7	55.017	13.121
7.5	4.868	5.48
8	116.16	3.857
8.5	2142.8	39.575
9	12473	8.856
9.5	97303	60.277
10	3895.2	77.119

Osteogenic Construct 3 Elastic Modulus Values

Position	Exponential Fit	Polynomial Fit
mm	kPa	kPa
0	13770	4.544
0.5	2.6692	2.089
1	10.104	5.805
1.5	67.021	6.387
2	953.42	4.544
2.5	114.47	32.858
3		
3.5	54.506	6.7241
4	2022.8	16.414
4.5	300.37	6.395
5	1274.7	88.873
5.5	1287.5	6.976
6	1.268	5.54
6.5	546.17	15.443
7	6.145	3.424
7.5	19.49	2.388
8	3584	85.346
8.5	2.242	5.299
9	11.341	5.929
9.5	2.669	2.089
10	3.9995	14.547

Basal Construct 1 Elastic Modulus Values

Position	Exponential Fit	Polynomial Fit
mm	kPa	kPa
0	41.601	68.525
0.5	36.983	1.777
1	166.7	69.437
1.5	131.52	1.51
2	23.898	0.542
2.5	169.3	1.2214
3	9.7815	1.3529
3.5	81.881	1.702
4	9.6214	0.2367
4.5		
5	45.304	0.4265
5.5	162.69	3.567
6	10.614	0.3647
6.5		
7	8.561	2.242
7.5	10.803	0.00736
8	10.607	0.9312
8.5	0.686	0.1673
9	13.304	0.9218
9.5	4.464	2.849
10	2.5012	1.416

Basal Construct 2 Elastic Modulus Values

Position	Exponential Fit	Polynomial Fit
mm	kPa	kPa
0	7.489	4.994
0.5	677.18	2.169
1	258.66	149.92
1.5	136.19	4.191
2	230.87	24.52
2.5	197.37	1.4062
3	315.14	2.1502
3.5	431.86	1.414
4	246.82	1.183
4.5	334.34	2.183
5	769.49	0.679
5.5	215.64	2.0296
6	370.17	1.997
6.5	228.31	4.0225
7	272.98	4.868
7.5	1622.6	3.162
8	552.34	26.01
8.5	218.28	21.049
9		
9.5		
10	1.269	1.328

References

1. A. D. L. Humphris, M. J. Miles, and J. K. Hobbs. (2005) A Mechanical Microscope: High-speed Atomic Force Microscopy. *University of Bristol, H.H. Wills Physics Laboratory Applied Physics Letters* **86**: 034106

2. A. Sarvazyan, O. Rudenko, S. Swanson, J. Fowlkes, and S. Emelianov, "Shear wave elasticity imaging: A new ultrasonictechnology of medical diagnostics," *Ultrasound Med. Biol.*, vol. 24, no. 9, pp. 1419–1435, 1998.

3. "Atomic Force Microscopy" *nanoScience Instruments*. Available (Online) http://www.nanoscience.com/education/AFM.html. Accessed May 5, 2009.

4. Bell E, Ivarsson B, Merrill C. "Production of a tissue-like structure by contraction of collagen lattices by human fibroblasts of different proliferative potential in vitro." *Proc Natl Acad Sci USA*; Vol. 76, 1979, pp. 1274–1278.

5. Bernacki SH, Wall ME, and Loboa EG. 2008. Isolation of human mesenchymal stem cells from bone and adipose tissue. Methods Cell Biol.;86:257-78.

6. Bercoff J, Chaffai S, Tanter M, et al. In vivo breast tumor detection using transient elastography. Ultrasound Med Biol 2003; 29:1387–1396.

7. Bonassar L.J., Vacanti C.A., "Tissue engineering: The first decade and beyond." *J Cell Biomchem* Vol. 30-31, 1998, pp297-303.

8. Bruder, S. P., Jaiswal, N., and Haynesworth, S. E. "Growth kinetics, self-renewal, and the osteogenic potential of purified human mesenchymal stem cells during extensive subcultivation and following cryopreservation. *J. Cell Biochem*. Vol. 64, 1997 pp. 278.

9. Catheline S, Gennison JL, Delon O, et al. Measurements of viscoelastic properties of homogeneous soft solid using transient elastography: an inverse problem approach. J Acoust Soc Am 2004; 116:3734–3741.

10. Chaudhuri, O., Parekh, S., Lam, W., Fletcher, D., "Combined Atomic Force Microscopy and Side-Vew Optical Imaging for Mechanical Studies of Cells." *Nature Methods* Vol 6. No. 5, May 2009.

11. Choi, J. R., "Approach to the Quantum Evolution for Underdamped, Critically Damped, and Overdamped Driven Harmonic Oscillators Using Unitary Transformation." *Reports on Mathematical Physics* Vol. 52, 2003, pp. 321-329

12. Cowin, S. C., He, Q. C., (2005). "Tensile and Compresive Stress Yield Criteria for Cancellous Bone". *Journal of Biomechanics.* **38**:141-144

13. Crandall, Dahl, Lardner (1959). *An Introduction to the Mechanics of Solids*. McGraw-Hill: New York.

14. Erkamp, R.Q., Wiggins, P., Shovoroda, A.R., Emelianov, S.Y., and, O'Donnel, M., (1998). "Measuring the Elastic Modulus of Small Tissue Samples." *Ultrasonic Imaging* **20**: 17-28.

15. F. Viola and W. F. Walker, "Radiation force imaging of viscoelasticproperties with reduced artifacts," *IEEE Trans. Ultrason.,Ferroelect., Freq. Contr.*, vol. 50, no. 6, pp. 736–742, 2003.

16. Gao L, Parker KJ, Lerner RM, Levinson SF. Imaging the elastic properties of tissue: a review. Ultrasound Med Biol 1996; 22:959–977.

17. Gedney, R,. "Tensile Testing Basics, Tips and Trends". *Quality Test and Inspection*. Admet Inc. January 2005.

18. Glozman, T., Azhari, H., "A Method for Characterization of Tissue Elastic Properties Combining Ultrasound Computed Tomography With Elastography." J Ultrasound Med. Vol. 29 pp 387-398.

19. Greenleaf JF, Fatemi M, Insana M. Selected methods for imaging elastic properties of biological tissues. Annu Rev Biomed Eng 2003; 5:57–78.

20. Halleux C, Sottile V, Gasser JA, Seuwen K. 2001. Multi-lineage potential of human mesenchymal stem cells following clonal expansion. *J Musculoskelet Neuronal Interact* 2: 71-76

21. Hishikawa K, Miura S, Marumo T, et al. "Gene expression profile of human mesenchymal stem cells during osteogenesis in three-dimensional thermoreversible gelation polymer. " *Biochem Biophys Res Comm.* Vol. 317, 2004, pp. 1103-1107

22. Hosford, W. F., Mechanical Behavior of Materials Second Edition. Cambridge University Press: New York, NY. 2010. pp 20-33.

23. Ikai, A., Afrin, R., (2003) Toward Mechanical Manipulations of Cell Membranes and Membrane Proteins Using an Atomic Force Microscopy. *Cell Biochemistry and Biophysics*. **39**: 257-277

24. Jaiswal, R. K., Jaiswal, N., Bruder, S. P., Mbalaviele, G.,Marshak, D. R., and Pittenger, M. F., "Adult human mesenchymal stem cell differentiation to the osteogenic or adipogenic lineage is regulated by mitogen-activated protein kinase." *J. Biol. Chem*. Vol. 275, 2000, pp. 9645.

25. Jensen, Jorgen. "Medical ultrasound imaging" Progress in Biophysics and Molecular Biology. Vol. 93 (2007) 153-165.

26. Jiles, D., (2008). Introduction to the Principles of Materials Evaluation. CRC Press: New York, NY. pp. 17-18.

27. Knott L and Bailey AJ. “Collagen cross-links in mineralizing tissues: a review of their chemistry, function, and clinical relevance.” *Bone*. Vol. 3, 1998, pp 181-187.

28. Krouskop, T. A., Wheeler, T. M., Kallel, F., Garra, B. S., Hall, T., (1998). “Elastic Moduli of Breast and Prostate Tissues Under Compression”. *Ultrasonic Imaging.* **20**: 260-274.

29. Lacroix D., and Prendergast P.J., A mechano-regulation model for tissue differentiation during fracture healing: Analysis of gap size and loading. *J. Biomech.* Vol. 32, 1999, pp. 255.

30. Lakes,Roderic, Viscoelastic Materials, Cambridge University Press 2008 pp. 1-5 New York, New York.

31. Lutz, H.T., Gharbi, H. A., Basics of Ultrasound. New York, NY. Spinger Berlin Heidelberg, 2006, pp1-19.

32. Lynnworth, L. C., E. P. Papadakis, K. A. Fowler, (1977) "Ultrasound Propagation Measurements and Applications," *International Advances in Nondestructive Testing*. **5**: 71-115.

33. Mauldin, F. W. Jr., Haider, M. A., Loboa, E. G., Behler, R. H., Euliss, L. E., Pfeiler, T. W., Gallippi, C. M., “Monitored Steady-State Excitation and Recovery (MSSER) Radiation Force Imaging Using Viscoelastic Models” *IEEE Transaction on Ultrasonics, Ferroelectrics, and Frequency Control*,Vol. 55, No. 7, 2008, pp. 1597-1610.

34. McCrum, N. G., "Principles of Polymer Engineering," Oxford University Press: 2003 pp. 117-122.

35. Meyer M. A., Chawla K.K., Mechanical Behavior of Materials. Prentice-Hall: Upper Saddle River, 1999, pp 98-103.

36. Momoh, J. J., Ajueyitsi, O.A., Onipede, A. M., (2008). “Development of a Low Cost Mechanically Operated Tensile and Creep Testing Machine.” *Journal of Engineering and Applied Sciences*. **6**: 491-495.

37. Mwanje, J., (1980). “An Approach to Hooke’s Law.” *Phys Educ.* **15**: 103-105.

38. Nightingale, K., McAleavey, S., Trahey, G., “Shear-Wave Generation Using Acoustic Radiation Force: *In Vivo* and *Ex Vivo* Results” Ultrasound in Med and Biol. Vol 29 No. 12, 2003, pp. 1715-1723.

39. Nightingale, K.R., Palmeri, M.L., Nightingale, R. W., Trahey, G. E., “On the feasibility of remote palpation using acoustic radiation force*.” J. Acoust. Soc Am* Vol. 110, 2001.

40. Nightingale, K., Soo, M. S., Nightingale, R., Trahey, G., “Acoustic Radiation Force Impulse Imaging: In Vivo Demonstration of Clinical Feasiblity.” *Ultrasound in Medicine and Biology*. Oct 24, 2001

41. Nyborg, W. Acoustic streaming. In: Mason, W., ed., Physical Acoustics, New York: Academic Press Inc, vol. IIB, chap. 11, 265{331. 1965.

42. (old 2.) Chaudhuri, O., Parekh, S., Lam, W., Fletcher, D., "Combined Atomic Force Microscopy and Side-Vew Optical Imaging for Mechanical Studies of Cells." *Nature Methods* Vol 6. No. 5, May 2009.

43. O'Neil P. V., Advanced Engineering Mathematics 6th edition. Thompson: Toronto, Ontario. 2007. pp. 93-106.

44. O. Rudenko, A. Sarvazyan, and S. Emelianov, "Acoustic radiation force and streaming induced by focused nonlinear ultrasound in a dissipative medium," *J. Acoust. Soc. Amer.*, vol. 99, no. 5, pp. 2791–2798, 1996.

45. Palmeri, M.L., Sharma, A. C., Bouchard, R. R., Nightingale, R. W., Nightingale, K. R., "A Finite-Element Method Model of Soft Tissue Response to Impulsive Acoustic Radiation Force." *IEEE Transaction on Ultrasonics, Ferroelectrics, and Frequency Control,* Vol 52. No. 10, 2005, Pp 1699-1711.

46. Pfeiler, T. W., Sumanasinghe, R. D., Loboa, E. G., "Finite element modeling of 3D human mesenchymal stem cell-seeded collagen matrices exposed to tensile strain." *Journal of Biomechanics* Vol. 41, 2008, pp. 2289-2296.

47. Pittenger, M.F., Mackay, A.D., Beck, S.C., Jaiswal, R. F., Douglas, R., Mosca, J.D., Moorman, M.A., Simonetti, D.W., Craig, S., Marshak, D. R., "Multilineage Potential of Adult Human Mesenchymal Stem Cells." *Science* Vol. 284(5411) pp. 143-147.

48. Prince, J. L., Links, J. M., Medical Imaging Signals and Systems. Pearson Prentice Hall: Upper Saddle River, NJ, 2006, Pp 11-12, 315-316.

49. Puttini, S., et. al. (2009) "Gene-mediated Restoration of Normal Myofiber Elasticity in Dystrophic Muscles." *The American Society of Gene Therapy*. **17**: 19-25.

50. Samani A, Plewes D. (2004) "A method to measure the hyperelastic parameters of ex vivo breast tissue samples." *Phys Med Biol*. **49**:4395–4405.

51. Sarvazyan A, Rudenko OV, Swanson SD, Fowlkes JB, Emelianov Y. 1998. Shear wave elasticity imaging: a new ultrasonic technology of medical diagnostics. *Ultrasound Med. Biol.* 24(9):1419–35

52. Sarvazyan A. (1993). Shear acoustic properties of soft biological tissues in medical diagnostics. *Proc. Acoust. Soc. Am.*, 125th, Ottawa, Canada, p. 2329

53. Singh, B. N., Tahtinen, S., Moilanen., Jacquet, P., Dekeyser, J., (2003). "In-reactor Uniaxial Tensile Testing of Pure Copper at a Constant Strain rate at 90˚C." *Journal of Nuclear Materials*. **320**: 299-304.

54. Sottile V, Halleux C, Bassilana F, Keller H, Seuwen K. Stem cell characteristics of human trabecular bone-derived cells. *Bone* Vol. 30, 1999, pp 699-704

55. Splung Physics.com "Damped Oscillations" Available (Online) http://www.splung.com/content/sid/2/page/damped_oscillations. Accessed March 12, 2010.

56. Stephen T. Thornton and Jerry B. Marion, *Classical Dynamics of Particles and Systems, 5th Edition*, California: Thomson Books/Cole 2004

57. Sumanasinghe RD, Osborne JA, Loboa EG. "Mesenchymal stem cell-seeded collagen matrices for bone repair: effects of cyclic tensile strain, cell density, and media conditions on matrix contraction in vitro." *J Biomed Mater Res A.* Vol. 88(3), 2009. pp. 778-86.

58. Sumanasinghe RD, Bernacki SH, and Loboa EG. "Osteogenic differentiation of human mesenchymal stem cells in collagen matrices: effect of uniaxial cyclic tensile strain on bone morphogenetic protein (BMP-2) mRNA expression." *Tissue Eng*. Vol 12. 2006, pp.3459-3465.

59. Taléns-Visconti, R., Bonora, A., Jover, R., Mirabet, V., Carbonell, F., Castell, J.V., and Gómez-Lechón, M.J., Hepatogenic differentiation of human mesenchymal stem cells from adipose tissue in comparison with bone marrow mesenchymal stem cells. *Shi Jie Wei Chang Bing Xue Za Zhi Ying Wen Ban.* 2006, Vol. *12*(36) pp. 5834.

60. Taylor LS, Porter BC, Rubens DJ, Parker KJ. Three-dimensional sonoelastography: principles and practices. Phys Med Biol 2000; 45:1477–1494.

61. Torr, G. The acoustic radiation force. Am. J. Phys. 52:402 408, 1984.

62. W. F. Walker, F. J. Fernandez, and L. A. Negron, "A method of imaging viscoelastic parameters with acoustic radiation force," *Phys. Med. Biol.*, vol. 45, no. 6, pp. 1437–1447, 2000

63. Wells, P. N., "Ultrasound imaging" Phys. Med. Biol. Vol. **51** (2006) pp. R83-R98

64. Woo, J., "A short history of the development of Ultrasound in Obstetrics and Gynecology". 2002. Available (Online) http://www.ob-ultrasound.net/history1.html. Accessed March 12, 2010

65. Xydeas T, Siegmann K, Sinkus R, Krainick-Strobel U, Miller S, Claussen CD. Magnetic resonance elastography of the breast: correlation of signal intensity data with viscoelastic properties. Invest Radiol 2005; 40:412–420.

66. "Young's Modulus (Elastic Modulus) – Strength (Mechanics) of Materials"*Engineers Edge"* Available (Online) http://www.engineersedge.com/material_science/youngs_modulus.htm. Accessed May 7, 2009.

67. Zill, D. G., Cullen, M. R., Differential Equations with Boundary-Value Problems.